

ESTCP Cost and Performance Report

(MR-201105)



High-Power Vehicle-Towed TEM for Small Ordnance Detection at Depth

February 2014

*This document has been cleared for public release;
Distribution Statement A*



ENVIRONMENTAL SECURITY
TECHNOLOGY CERTIFICATION PROGRAM

U.S. Department of Defense

COST & PERFORMANCE REPORT

Project: MR-201105

TABLE OF CONTENTS

	Page
EXECUTIVE SUMMARY	ES-1
1.0 INTRODUCTION	1
1.1 BACKGROUND	1
1.2 OBJECTIVE OF THE DEMONSTRATION	2
1.3 REGULATORY DRIVERS	2
2.0 TECHNOLOGY	3
2.1 TECHNOLOGY DESCRIPTION	3
2.2 ADVANTAGES AND LIMITATIONS OF THE TECHNOLOGY	5
3.0 PERFORMANCE OBJECTIVES	8
4.0 SITE DESCRIPTION	10
4.1 SITE SELECTION	10
4.2 SITE HISTORY	10
4.3 SITE GEOLOGY	11
4.4 MUNITIONS CONTAMINATION	12
5.0 TEST DESIGN	14
5.1 CONCEPTUAL EXPERIMENTAL DESIGN	14
5.2 SITE PREPARATION	15
5.3 SYSTEM SPECIFICATIONS	15
5.4 DATA COLLECTION	15
5.5 VALIDATION	16
6.0 DATA ANALYSIS PLAN	18
6.1 PREPROCESSING	18
6.2 TARGET SELECTION FOR DETECTION	18
6.3 PARAMETER ESTIMATION	19
6.4 CLASSIFICATION AND TRAINING	19
6.5 DATA PRODUCTS	20
7.0 PERFORMANCE ASSESSMENT	22
7.1 WEST JEFFERSON OVERVIEW	22
7.2 APG OVERVIEW	24
7.2.1 Calibration Grids	24
7.2.2 Blind Grid	29
7.2.3 Small Target Grid	32
7.2.4 Analysis	37
7.2.5 Conclusions	39

TABLE OF CONTENTS (continued)

	Page
8.0 COST ASSESSMENT	40
8.1 COST MODEL	40
8.2 COST DRIVERS	41
8.3 COST BENEFITS.....	42
9.0 IMPLEMENTATION ISSUES	44
10.0 REFERENCES	46
APPENDIX A POINTS OF CONTACT.....	A-1

LIST OF FIGURES

		Page
Figure 1.	Theoretical model of primary and secondary EM fields (a) and photo of Battelle airborne TEM-8 system (b).	3
Figure 2.	Schematic (a) and photo (b) of the TEM-8g system.....	4
Figure 3.	Plots of measured and modeled EM response across the array (receivers 1-8) over vertical and horizontal 20mm targets from Camp Sibert field test.	7
Figure 4.	GoogleEarth image of West Jefferson UXO Test Grid (green trapezoidal field).....	10
Figure 5.	GoogleEarth image of APG Standardized Test Grid areas (blue).	11
Figure 6.	Signal attenuation due to altitude (offset) for a 20mm projectile.	19
Figure 7.	Thumbnail plots of the Bin2 response for the NS (left) and EW (right) survey lines at the West Jefferson Grid.	22
Figure 8.	Plot of secondary versus primary polarizability amplitude for ground truth seeds at West Jefferson Grid.....	23
Figure 9.	Plot of primary polarizability decay power versus amplitude for ground truth seeds at West Jefferson Grid.	23
Figure 10.	Plot of Bin2 response at APG Calibration Grid.....	25
Figure 11.	Plot of Bin2 response at APG Calibration Grid.....	25
Figure 12.	Overlapping contours of measured and modeled (from inverted target) results of 2-dipole models for anomalies in Calibration Grid Cells F4 (25mm), G1 (37mm) and G4 (37mm).	26
Figure 13.	Calibration Grid location error plot.	27
Figure 14.	Plot of secondary versus primary polarizability amplitude for calibration items.....	28
Figure 15.	Plot of primary polarizability decay power versus amplitude for calibration items.....	29
Figure 16.	Plot of Bin2 response at APG Calibration Grid.....	30
Figure 17.	(a-left) Plot of secondary versus primary polarizability amplitude and (b-right) primary polarizability decay power versus amplitude.	31
Figure 18.	ROC curve for TEM-8g at Blind Grid.....	32
Figure 19.	Plot of Bin2 response at APG Calibration Grid after removal of background susceptibility.	33
Figure 20.	(a-left) Plot of secondary versus primary polarizability amplitude and (b-right) primary polarizability decay power versus amplitude.	34
Figure 21.	(a-left) ROC curve from Battelle list, Small Target Grid, capped cells, all ordnance types, depths to 20x diameter. (b-right) ROC curve from SAIC list, Small Target Grid, capped cells, all ordnance types, depths to 20x diameter.....	35
Figure 22.	(a-top left) ROC curve from Battelle list, Small Target Grid, <i>uncapped</i> cells, all ordnance types, depths to 20x diameter. (b-top right) ROC curve from Battelle list, Small Target Grid, capped cells, <i>37mm and 40mm</i> ordnance types, depths to 20x diameter. (c-bottom left) ROC curve from Battelle list, Small Target Grid, <i>uncapped, 37mm and 40mm</i> ordnance types, depths to 20x diameter.....	36

LIST OF TABLES

	Page
Table 1.	Performance objectives. 8
Table 2.	Project Gantt chart. 14
Table 3.	Averaged inversion results forming initial TEM-8g library. 23
Table 4.	Cost model metrics. 40
Table 5.	Productivity statistics for a variety of detection and classification instruments. 42

ACRONYMS AND ABBREVIATIONS

2D	two-dimensional
APG	Aberdeen Proving Ground
ATC	Aberdeen Test Center
DGPS	differential global positioning system
EM	electromagnetic
ESTCP	Environmental Security Technology Certification Program
FKPBR	Former Kirtland Precision Bombing Range
FP	false positive
GPO	geophysical prove-out
GPS	global positioning system
ha	hectare
HEAT	high-explosive anti-tank
Hz	hertz
ID	identification
IVS	instrument verification strip
m/s	meters per second
mV	millivolt
Pcc	probability of clutter classification
Pd	probability of ordnance detection (above detection threshold)
Pdisc	probability of ordnance discrimination (properly classified by type)
ppm	parts per million
PPS	pulse per second
QC	quality control
ROC	receiver operating characteristic
Rx	receiver coil (orientation independent)
SNR	signal to noise ratio
TEM	time-domain electromagnetic
Tx	transmitter coil (orientation independent)
UXO	unexploded ordnance

This page left blank intentionally.

ACKNOWLEDGEMENTS

The authors would like to express their thanks to Mr. Robert Selfridge of the U.S. Army Engineering Support Center, Huntsville, for the initial suggestion to develop this system and his subsequent support of the initial feasibility testing and calibration testing at Camp Sibert.

We would also like to thank Dr. Scott Holladay at Geosensors, Inc., and Dr. Bruce Barrow at Leidos (formerly SAIC) for their contributions to the hardware and inversion software respectively.

*Technical material contained in this report has been approved for public release.
Mention of trade names or commercial products in this report is for informational purposes only;
no endorsement or recommendation is implied.*

This page left blank intentionally.

EXECUTIVE SUMMARY

The objective of this project was to demonstrate the performance of an electromagnetic (EM) system optimized for detection of small ordnance targets, such as 20 millimeter (mm) and 37mm projectiles, at depths greater than the standard “11x diameter” metric currently employed. The performance goal for this project was 20x the target diameter. Classification of targets was not an expressed objective of the project, except that considerable non-ordnance items of this size were expected to be detected by the system, so an approach for excluding these items from dig lists was needed. Classification of the sort demonstrated by cued instruments was beyond the expected capabilities of the data produced by this instrument. Ultimately, classification using inversion polarizabilities proved both possible and effective by utilizing bi-directional (orthogonal) surveying.

A total of four field operations were carried out. The first was a feasibility study using the one half of the existing airborne system without modification. The second was an initial shake-down of the modified system to determine the optimal field settings (base frequency, survey speed, platform configuration, transmitter power, vehicle offset, filter parameters, etc.). The third was a preliminary field test to ensure proper operability of the system at the specified settings before the fourth and final demonstration.

The initial feasibility study was conducted prior to the contract award. The feasibility study and initial shake-down were both conducted at the Camp Sibert Geophysical Prove Out (GPO) grid with the assistance of the U.S. Army Engineering Support Center, Huntsville. The preliminary field test was conducted at Battelle’s West Jefferson, Ohio Unexploded Ordnance (UXO) Test Grid. The final demonstration was conducted at the Aberdeen Proving Ground (APG) Geophysical Test Center.

This project met all of the original expectations for small target detection at depth, and greatly exceeded expectations in terms of discrimination and classification by combining orthogonal survey data. For the medium and large targets at normal depths (25mm-105mm down to 11x diameter), results were nearly perfect with a vertical receiver operating characteristics (ROC) curve. For the small targets at greater depths (20mm-40mm down to 20x diameter) all targets were detected at depths down to 20x diameter burial depth (probability of ordnance detection [Pd] 100%), and all except the 20mm targets could be discriminated with 100% probability of ordnance discrimination (Pdisc). The 20mm targets had Pdisc reduced to 0.87/0.90 (capped/uncapped), primarily at the greater depths. The ROC curve for these was very good, but not as vertical as for the medium/large targets. Classification of clutter (probability of clutter classification [Pcc]) was slightly lower than the corresponding Pdisc, reflecting a cautious approach to declarations. Pcc was 0.87 in the Blind Grid, and 0.52/0.61 in the Small Target Grid. This last metric was the only one that came close to falling below the design expectations of 0.60. All metrics surpassed those of the existing technology benchmark (EM-61 array). Originally intended purely as a detection tool and replacement for the standard EM-61 array, this system has demonstrated superior depth detection and comparable discrimination capabilities to other dynamic classification tools as demonstrated at the APG site.

This page left blank intentionally.

1.0 INTRODUCTION

The objective of this project was to demonstrate detection of small ordnance targets, such as 20 millimeter (mm) and 37mm projectiles, at depths greater than the standard “11x diameter” metric currently employed. This will reduce the cost and improve the reliability of remedial actions. The technology being demonstrated was an extension of the Battelle airborne time-domain electromagnetic (TEM)-8 electromagnetic (EM) system. The essential electronics and data acquisition system remained the same, but the transmitter and receiver configurations were optimized for these specific targets based on theoretical modeling results. This report details the feasibility study, optimization modeling, field testing and demonstration of the new TEM-8g system.

1.1 BACKGROUND

The detection of very small ordnance items (e.g., 20mm and 37mm projectiles) is difficult due to the low amplitude magnetic and EM response of such items. The standard rule for maximum burial detection depth is 11x the target diameter. Several factors alter actual performance including ground clearance of the instrument. This is particularly true for small targets where the ground clearance becomes a relatively large percentage of the total offset distance. Detection depths for standard instruments (e.g., EM-61 arrays) are therefore typically limited to approximately 0.41 meter (m) for 37mm (11x diameter), but only about 0.15m for 20mm (8x diameter) (Nelson, et al., 2009). The magnetic response is often comparable to that of local geologic and soil response. The EM response is relatively immune to geology, but standard instruments do not produce sufficient power to energize such small targets above background noise, especially at late times. The combination of low signal-to-noise and a lack of sufficient “look-angles” with standard instruments makes target classification difficult. Also, the spatial resolution of standard sensors, particularly across-line, may be too coarse to reliably or accurately locate individual small or weak targets, even with sensor arrays.

This new system is a ground-based version of the successful Battelle TEM-8 airborne EM sensor platform. It features a single large transmitter with eight small receivers on a vehicle-towed platform. It differs from existing technologies primarily in its focus on detecting the response from small and deep targets by maximizing the power of the transmitter field and the resolution of the receivers. The more powerful transmitter field increases the probability that the target response will exceed the noise threshold and decreases the variability of that response, all leading to higher detection capabilities.

There are several benefits to the new system. Classification of the quality demonstrated by cued instruments was beyond the expected capabilities of this instrument because of the lack of multiple “look-angles” at the target. Ultimately, classification using inversion polarizabilities proved both possible and effective by combining orthogonal survey data. In addition to the increased peak response, the rectangular transmitter produces sufficiently strong horizontal fields to enable multiple look-angles and subsequent polarizability inversion of the measured data. These inversion results can be used to discriminate clutter from ordnance, and to classify ordnance by type, thereby reducing the number of false positive excavations.

By increasing the detection depth for these targets, remedial actions will not have to be conducted in “lifts” with successive geophysical surveys, reacquisitions and removals at 6-inch depth intervals. The improved classification can reduce the overall number of excavations required. The net result is higher efficiency and reduced cost for ordnance clean up for these typically difficult targets.

1.2 OBJECTIVE OF THE DEMONSTRATION

The objective of this project was to demonstrate the performance of an EM system optimized for detection of small ordnance targets, such as 20mm and 37mm projectiles, at depths greater than the standard “11x diameter” metric currently employed. The performance goal for this project was 20x the target diameter. Classification of targets was not an expressed objective of the project, except that considerable non-ordnance items of this size were expected to be detected by the system, so an approach for excluding these items from dig lists was needed. No other instruments have been rigorously tested for detection of 20mm projectiles or for detection of larger ordnance at depths greater than 11x diameter. Without a prior point of comparison, objective demonstration criteria were extrapolated from published performance results and design expectations.

1.3 REGULATORY DRIVERS

There are no known regulatory drivers relevant to the acceptance and use of this technology.

2.0 TECHNOLOGY

The technology demonstrated was a ground-based extension of the Battelle TEM-8 airborne time-domain EM system, named the TEM-8g. The success of the airborne system at detecting ordnance at large offsets prompted the development of a ground-based system to detect small ordnance items at greater depths than had been previously possible.

2.1 TECHNOLOGY DESCRIPTION

The technology is based on the principles of time-domain EM theory. Current through a transmitter loop generates a secondary EM field within a metallic target. When the current is shut off rapidly, the decay of the secondary field is measured at different locations by a receiver coil (Figure 1a).

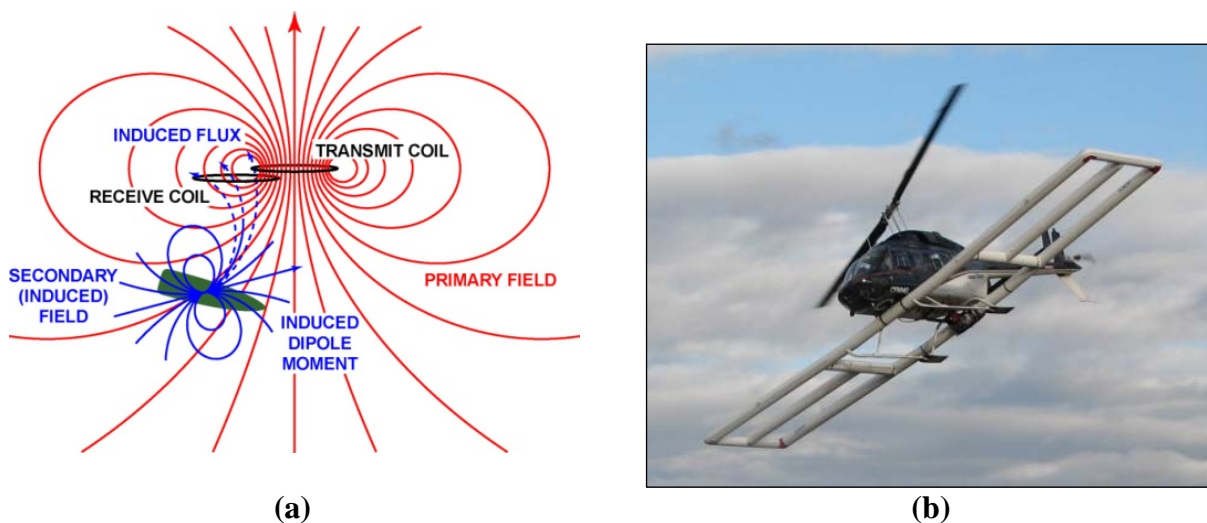


Figure 1. Theoretical model of primary and secondary EM fields (a) and photo of Battelle airborne TEM-8 system (b).

The airborne predecessor to the current instrument was developed with Environmental Security Technology Certification Program (ESTCP) support between 2001 and 2004 under project MM-200101. Internal Battelle research funds were used to extend the prototype system to a production capable system, the TEM-8. A subsequent ESTCP-supported demonstration of the Battelle TEM-8 airborne system was conducted between 2008 and 2009 under ESTCP project MM-0743 (Figure 1b). Results from TEM-8 airborne tests at Battelle's Unexploded Ordnance (UXO) Test Site near Columbus, Ohio showed a probability of ordnance detection (Pd) of 53% for 60mm mortars at an average 2m sensor height. Improvements were made to the TEM-8 system subsequent to the Ohio test, and prior to a demonstration at the Former Kirtland Precision Bombing Range (FKPBR), New Mexico in 2009. Results from this blind-seeded test at FKPBR showed a 99% Pd for buried targets as small as 81mm mortars for similar flight altitudes.

The ground-based version of Battelle's TEM-8 (Figure 2) uses the same electronic instrumentation as the airborne system with a modified transmitter and receiver configuration. Physics-based modeling was used to determine the optimum size of the receivers. The optimal combination of resolution and response amplitude was obtained when the receiver size was

approximately the same as the offset between the target and the center of the receiver. Smaller receivers had lower response amplitude without improved resolution. Larger receivers had higher amplitudes (up to a point) but degraded resolution due to averaging too much background. To maximize resolution for surface targets given a nominal ground clearance of approximately 20 centimeters (cm), a receiver diameter of 20cm was adopted. The transmitter size was then optimized to produce the largest possible peak response and uniform amplitude at each receiver across the array. A square transmitter produced a strong response from deep targets, but a rectangular transmitter produced more uniform results from surface targets. A range of transmitter shapes were modeled with length:width ratios between 1:1 and 6:1. Ultimately, a size of 2.5 m x 0.75m (3.3:1) was chosen as a compromise between near-surface symmetry and deep signal strength.

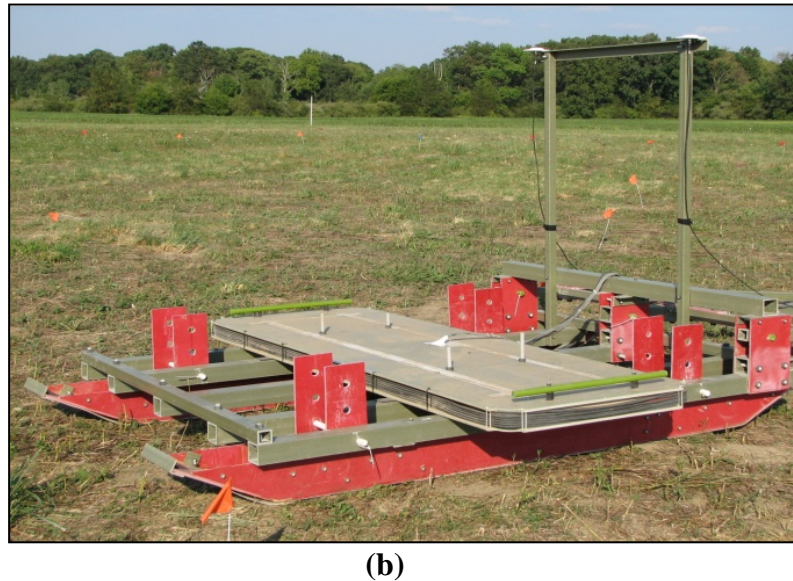
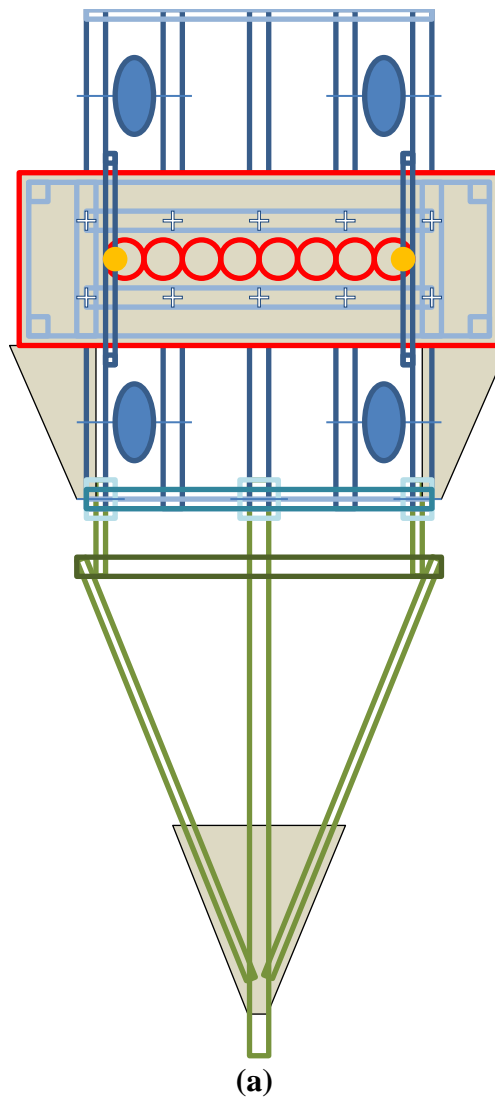


Figure 2. Schematic (a) and photo (b) of the TEM-8g system.

Red lines on schematic show transmitter and receiver coils. Schematic shows wheeled option; photo shows ski option. Sled option not shown.

After completion of the modeling task, the transmitter and receiver array were constructed and deployed in a brief field test to establish the basic operating parameters. This was conducted at the Camp Sibert Geophysical Prove out (GPO) grid. Based on these tests, a set of operating parameters was established to produce the optimal signal:noise. The first is the transmitter power, which was established at 60A and 12 coil turns. This maximized the response amplitude from deep targets, but retained a sufficiently fast current shut-off that early time data were not lost. The second parameter was using the base frequency, set at 30 hertz (Hz), to maximize the off-time decay. Sensor height was optimized by being as close to the ground as possible, although this may increase the response from the magnetic susceptibility of the soil. The wheeled platform proved easier to tow (less friction) but tended to bounce, especially at speeds in excess of 2 meters per second (m/s). The skis were more difficult to tow but produced a smoother ride. The tow vehicle contained the motor, the console and the electrical generator. An offset of >4m from the vehicle to the sensors was required for the vehicle noise to drop below the static instrument noise.

Static tests demonstrated detection of a 20mmP at 100cm offset with a 10:1 signal:noise ratio (SNR). In dynamic tests, the 20mmP were only detectable to 40cm depth (60cm offset) due to the increased noise from motion and background soil response. Response profiles varied depending on the target orientation. Vertical targets demonstrated a single peak signature, whereas horizontal targets aligned in the direction of travel demonstrated a double peak. Horizontal targets aligned perpendicular to the direction of travel demonstrated a single peak with an amplitude comparable to the local minimum between the double peaks of a transverse target. Measured results fit extremely well with modeled data.

Inversion of single-pass data showed that the primary polarizabilities were well defined, but the secondaries were rather poor due to the lack of orthogonal look angles. No orthogonal survey data were acquired as part of this field test. Calibration of the instrument response data and the dipole inversion algorithms were developed by SAIC based on this and subsequent field tests.

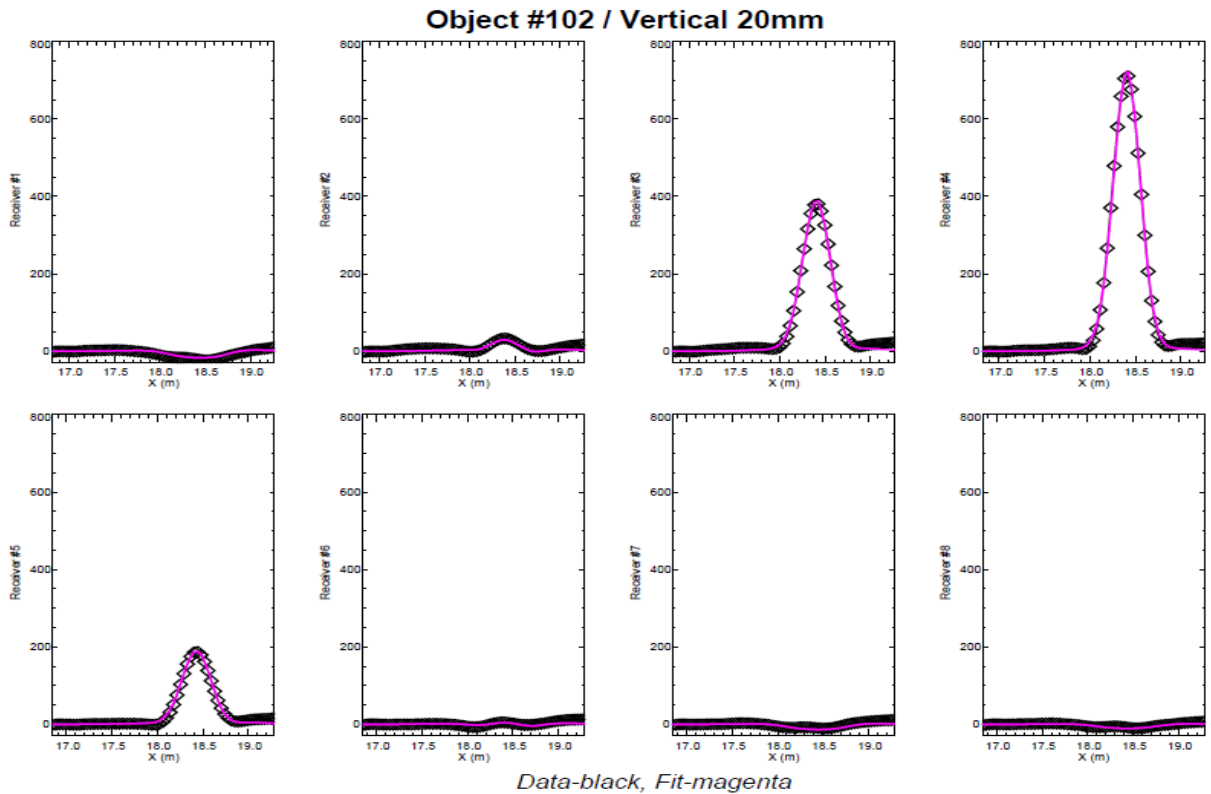
Therefore, TEM-8g therefore consists of a single high-power Z-axis transmitter 2.5m x 0.75m in size (Figure 2a). Eight 0.20m diameter Z-axis receivers are set out in a line on 0.22m centers forming an array 1.75m wide along the center of the transmitter. Data are sampled at 30Hz and the array is towed behind a utility vehicle at approximately 1.5m/s. The result is a high-resolution (0.22m x 0.05m) dataset that can be processed and gridded using the same basic tools as the standard EM61 (filter, level, grid). Unlike the EM61, however, the results can be used for effective inversion if bi-directional (orthogonal) survey data are available.

Positioning is provided by post-processed differential global positioning system (DGPS). Platform orientation is provided by multiple global positioning system (GPS) antennas and a moving baseline calculation. Nominal accuracy is 0.02m for the GPS antenna location and 0.1 degree for pitch/roll/heading.

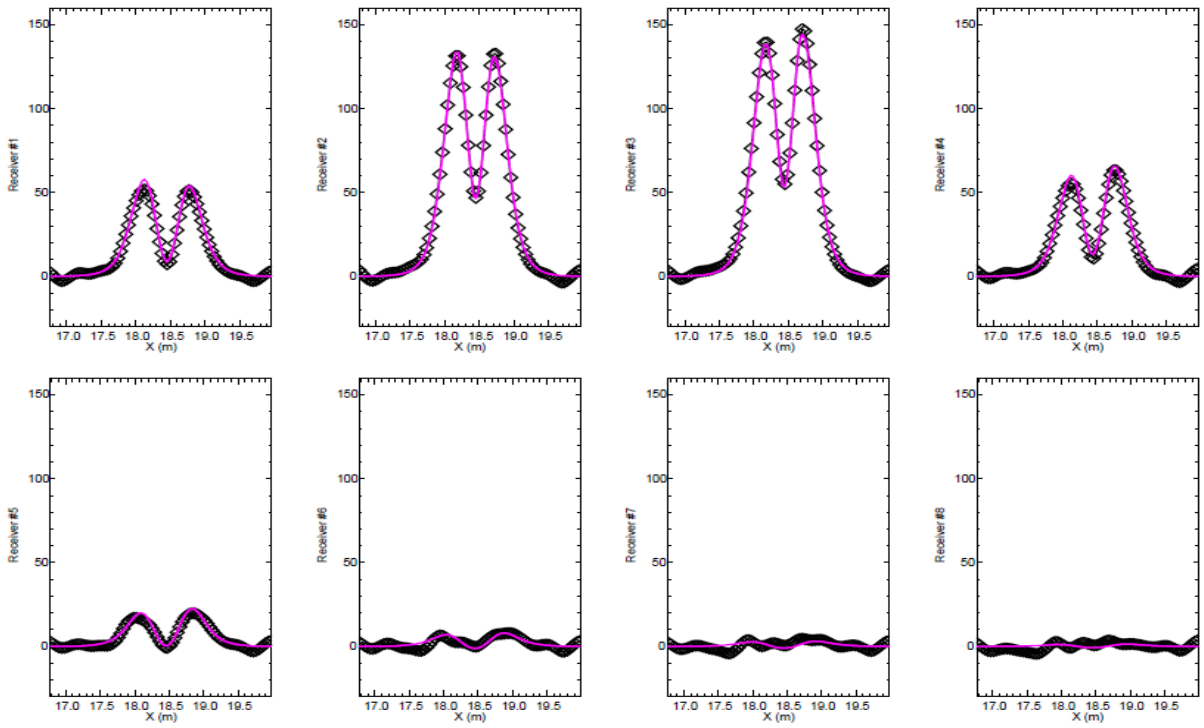
2.2 ADVANTAGES AND LIMITATIONS OF THE TECHNOLOGY

The industry standard technology for this application is an array of Geonics EM61-Mk2 sensors. Like the TEM-8g, the EM61 is a mono-static time-domain EM sensor, but consists of a single transmitter with a single receiver of the same size. Arrays of three EM61 sensors are common.

These fire and record each sensor in sequence across the array. The advantages of the TEM-8g system as compared to the EM61-MK2 include: (a) higher transmitter power, response amplitudes and signal:noise at depths between 0-1m, (b) digital rather than analog filters; (c) higher resolution receiver configuration (eight receivers at 20cm rather than 1 at 100cm) improves detection, positioning and inversion results for shallow targets, (d) wider swath width; (e) variable sample rate (user selection) to optimize for local background noise sources and (f) reliable discrimination and classification capabilities. The limitation of the TEM-8g is that it is not readily configurable into a man-portable system due to the higher power requirements. As with other towed arrays, it is typically not amenable to surveying in densely wooded or vegetated areas, or on steep slopes.



Object #101 / Horizontal 20mm



Data-black, Fit-magenta

Figure 3. Plots of measured and modeled EM response across the array (receivers 1-8) over vertical and horizontal 20mm targets from Camp Sibert field test.

3.0 PERFORMANCE OBJECTIVES

Performance objectives for the demonstration at Aberdeen Proving Ground (APG) and success levels for each objective are summarized in Table 1.

Table 1. Performance objectives.

Green, yellow and red cells reflect the level of success in meeting the stated objective.

Performance Objective	Metric	Data Required	Success Criteria	Results
Quantitative Performance Objectives				
Detection of med/large munitions at current detection depths to 11x diameter (blind grid)	Percent detected of seeded items (response stage)	<ul style="list-style-type: none"> Prioritized dig list Analysis of blind grid 	Design Pd=1.00 Current Pd=1.00	1.00
Detection of small munitions at current detection depths to 11x diameter (small target grid) (0-0.2m for 20-mm, 0-0.4m for 37-mm)	Percent detected of seeded items (response stage)	<ul style="list-style-type: none"> Prioritized dig list Analysis of small target grid 	Design Pd=0.95 Current Pd=0.75	1.00
Detection of small munitions at deeper detection depths to 20x diameter (small target grid) (0.2-0.4m for 20-mm, 0.4-0.75m for 37-mm)	Percent detected of seeded items (response stage)	<ul style="list-style-type: none"> Prioritized dig list Analysis of small target grid 	Design Pd=0.85 Current Pd=0.00	1.00
Classification of med/large munitions at current detection depths to 11x diameter (blind grid)	Percent of correctly classified items (discrim stage)	<ul style="list-style-type: none"> Prioritized dig list Analysis of blind grid 	Design Pdisc=0.80 Current Pdisc=0.50	1.00
Classification of small (37mm/40mm) munitions at deeper detection depths to 20x diameter (small target grid)	Percent of correctly classified items (discrim stage)	<ul style="list-style-type: none"> Prioritized dig list Analysis of small target grid 	Design Pdisc=0.70 Current Pdisc=0.25	1.00/1.00 (cap/uncap)
Classification of small (20mm) munitions at deeper detection depths to 20x diameter (small target grid)	Percent of correctly classified items (discrim stage)	<ul style="list-style-type: none"> Prioritized dig list Analysis of small target grid 	Design Pdisc=0.60 Current Pdisc=0.00	0.87/0.90 (cap/uncap)
Classification of clutter against med/large munitions at current detection depths to 11x diameter (blind grid)	Percent of clutter items declared as clutter (discrim stage)	<ul style="list-style-type: none"> Prioritized dig list Analysis of blind grid 	Design Pcc=0.80 Current Pcc=0.50	0.87
Classification of clutter against small munitions at deeper detection depths to 20x diameter (small target grid)	Percent of clutter items declared as clutter (discrim stage)	<ul style="list-style-type: none"> Prioritized dig list Analysis of small target grid 	Design Pcc=0.60 Current Pcc=0.00	0.52/0.61 (cap/uncap)
Location accuracy	Average error and standard deviation of depth estimates for seed items	<ul style="list-style-type: none"> Location of seed items Estimated location from analysis of geophysics data)Z <0.10 m ΦZ <0.10 m)0.05m Φ0.04m
Production rate	Number of acres of data collection per day	<ul style="list-style-type: none"> Log of field work and data analysis time accurate to 15 minutes 	Survey 1 acre/hour (or 0.5 acre/hour with bi-dir surveying)	0.73 acre/hour (0.36 acre/hour with bi-dir surveying)

Table 1. Performance objectives (continued).

Green, yellow and red cells reflect the level of success in meeting the stated objective.

Performance Objective	Metric	Data Required	Success Criteria	Results
Qualitative Performance Objectives				
Ease of use		<ul style="list-style-type: none"> Feedback from technician on usability 		Comparable to EM61 array

The TEM-8g is a new EM system which does not have a performance baseline from which success criteria could be derived. Two metrics were therefore presented for most objectives. One was the current performance metric of the closest available technology – the Geonics EM61-MK2. The second was the design objective of the Battelle project team. The final evaluation is whether the performance exceeded the industry standard and/or the design objectives.

Design objectives were set by the Battelle project team based on initial field test measurements. Metrics for the EM61-MK2 were drawn from the ESTCP live-site demonstration results at San Louis Obispo for the medium and large targets, and from the ESTCP Camp Butner demonstration for the small targets. However, there is only general correlation between these demonstrations and the objectives listed here for APG. Neither site included 20mm targets. For example, the San Louis Obispo site had mostly medium sized targets (no large, no small), whereas the Camp Butner site included 37mm, 105mm and 155mm projectiles, but no 20mm projectiles at any depth. Therefore, detection and classification metrics for the current state of the art are considered reasonable estimates based on published results, but may not fully represent the targets assessed in this project.

Classification metrics for the APG Small Grid are divided into capped and uncapped subgroups, reflecting ESTCP’s seeding of additional surface clutter items in some of the cells. The uncapped group replicates the standard seeding procedure used throughout the APG demonstration facility where the area around the target has been cleared of all metallic debris. The capped group has deliberate clutter items placed directly on top of the target location in order to mask the signature and make classification more difficult. This is closer to what may be presumed to be found in a live-site situation rather than a typical controlled test plot.

4.0 SITE DESCRIPTION

4.1 SITE SELECTION

Two demonstration sites are included in this report. The first is the Battelle UXO Test Grid in West Jefferson, Ohio. This site was used to conduct a shakedown survey of the new system prior to the final demonstration at the Standardized UXO Technology Demonstration Site at APG, Maryland. The results from the APG demonstration were used to assess system performance addressed in Section 3.

4.2 SITE HISTORY

The West Jefferson site (6 acres) was originally established in 2006 to test the detection capabilities of the Battelle airborne geophysical systems. It includes 73 targets ranging in sizes from 60mm mortars to 155mm projectiles at depths from near surface to 11x the target diameter. Prior to the shakedown survey, an additional 49 targets were added representing small munitions for this test. These included 20mm projectiles, 37mm projectiles, and 20mm-sized frag. Burial depths were between 5x and 20x the target diameter.

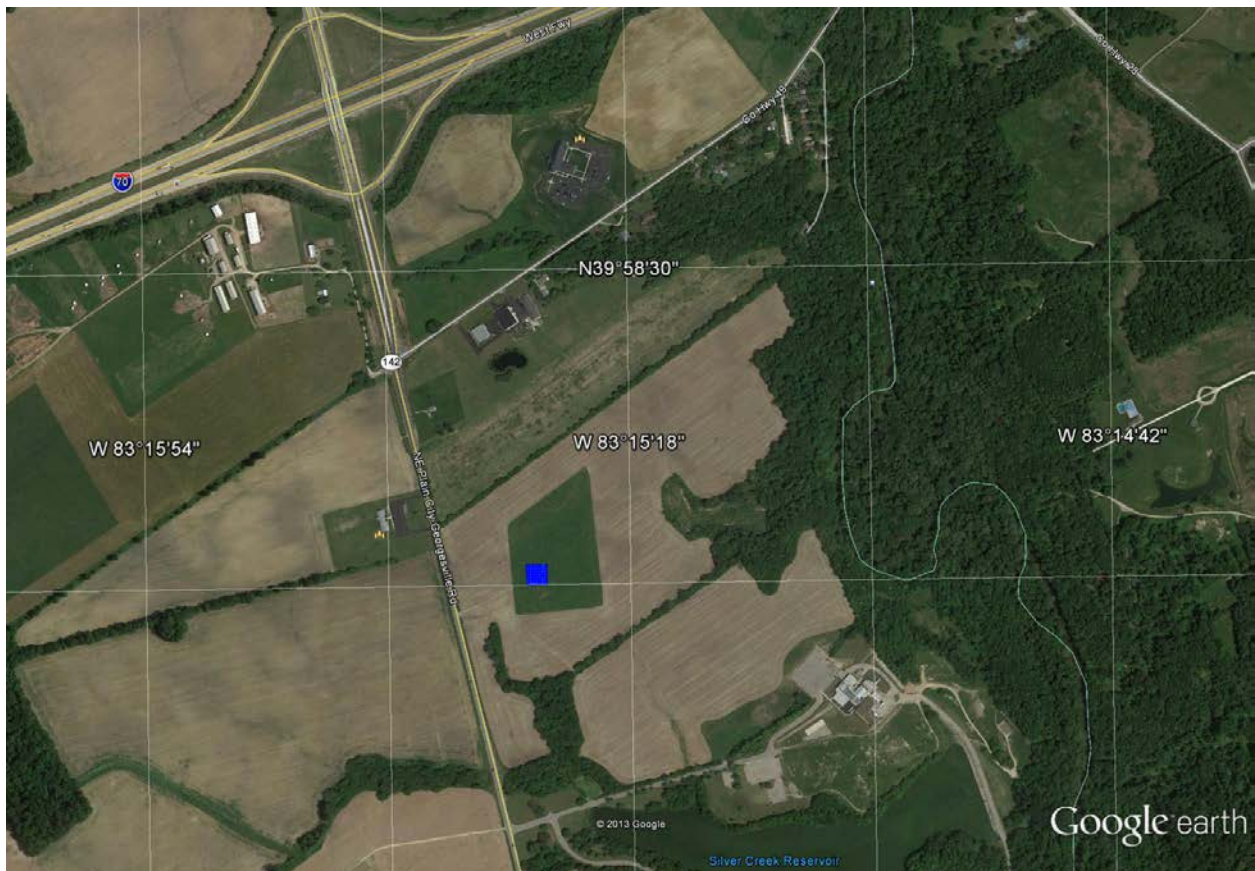


Figure 4. GoogleEarth image of West Jefferson UXO Test Grid (green trapezoidal field).

Small munitions sub-area is shown in blue.

Map shows intersection of interstate I-70 and Ohio State Route 142 for reference.

The final demonstration site included four areas of the Standardized UXO Technology Demonstration Site at APG. These were: Calibration Grid (0.30 acres), Small Calibration Grid (0.03 acres), Blind Grid (0.40 acres), and Small Target Grid (0.70 acres). The site topography was extremely flat and the vegetation included mowed grass and dirt. Apart from the Calibration Grid, no instrument verification strip (IVS) had been emplaced. There was a single sandy pit near the Calibration Grid that was used for clean background measurements. The Small Target Grid is the newest addition to the site and has not been used by any other contractor.



Figure 5. GoogleEarth image of APG Standardized Test Grid areas (blue).

4.3 SITE GEOLOGY

The geology in the West Jefferson, Ohio area consists of a glacial till layer, typically 50-200 ft thick, overlying Silurian age carbonate bedrock. The glacial till layer contains rocks with a wide variety of compositions and sizes, some of which can generate significant anomalies at the site.

Background geology at APG is composed predominantly of sandy soils with minimal magnetic background interference. The extent of conductive interference from possible salt water intrusion is minimal. The magnetic soil susceptibility is also minimal except in the Small Target Grid area where it is moderately strong.

4.4 MUNITIONS CONTAMINATION

The West Jefferson, Ohio site is clear of ordnance apart from seed items. Larger clutter items or items associated with larger magnetic responses were cleared when the grid was first established. There remains a band of magnetic and conductive clutter that runs NE-SW across the top third of the site. This was largely avoided during seeding. In addition, new clutter is occasionally added in the form of aluminum cans that are often shredded by mowing machines and widely scattered.

The APG site is assumed to be clear of ordnance except for seed items. Clutter densities are extremely low on all areas except the Small Target Grid, which is extremely cluttered and resembles a live-site location. Only a small radius of approximately 1m around the seed items has been cleared on the Small Target Grid. The ESTCP Program Office placed additional clutter items on the surface of the Small Target Grid prior to the demonstration. The other grids have been cleared of all original clutter, although anecdotal evidence suggests that the fill used was not perfectly clean and several small background anomalies remain.

This page left blank intentionally.

5.0 TEST DESIGN

5.1 CONCEPTUAL EXPERIMENTAL DESIGN

This project was conducted in several phases. The first phase included a detailed assessment of the feasibility study performed prior to this project, followed by modeling and design to optimize the transmitter and receiver configuration. The second phase involved building the coils and testing the performance of various firmware settings against buried targets at the Camp Sibert UXO GPO in Alabama. From these results, a final set of operating parameters and field procedures were developed. These were tested in phase three with two field demonstrations. The first was a shakedown test of the equipment and processing routines at Battelle's UXO Test Grid in West Jefferson, Ohio. The second was the final ESTCP demonstration at the Standardized UXO Test Site at APG, Maryland.

The experimental design of the field demonstrations was to seed and survey an area followed by data processing and analysis. For the West Jefferson study, seeding was conducted by Battelle and all targets were known to the investigators. These data were used as the primary training set for small targets (20mm projectiles, 37mm projectiles, small frag). For the APG demonstration, four different grids were used. Two were calibration grids of known targets, while two were blind grids. The calibration grid data were used as training sets for the two blind grids. The nominal center of each cell in the blind grids was known, but not the content of the cell or the exact target location (if any). There were no double-blind tests. A dig list was created for the blind grids, which included a declaration for each cell (anomaly or blank). If an anomaly was detected, the data were inverted and classified. The final dig list was submitted to ESTCP for third party analysis. Final statistics on the results were provided to the demonstration team for inclusion in this report.

Table 2. Project Gantt chart.

Phase and Task	4-6/11	7-9/11	10-12/11	1-3/12	4-6/12	7-9/12	10-12/12	1-3/13	4-6/13	7-9/13
Contract award	x									
Subcontracts issued	x									
Feasibility analysis		x								
Optimization modeling		x	x							
Build coils			x	x						
Camp Sibert field test				x						
Camp Sibert data analysis				x	x	x				
West Jefferson field test						x				
West Jefferson data analysis						x	x			
APG calibration survey							x			
APG calibration analysis							x	x		
APG small target survey									x	
APG small target analysis									x	x
Final reporting										x

5.2 SITE PREPARATION

The APG site was prepared entirely by ESTCP. The West Jefferson site was prepared by Battelle. The West Jefferson site was mowed and a pre-seed survey was conducted to locate existing anomalies to be removed or avoided. Several pieces of scrap were removed. Seed items were selected and placed at depths from 5x to 20x the target diameter (10cm – 40cm for 20mmP, 15cm-70cm for 37mmP). Locations and depths were recorded to within 2cm accuracy.

5.3 SYSTEM SPECIFICATIONS

The basic sensor system is identical to Battelle's airborne TEM-8, except that the transmitter and receiver coil specifications have been optimized for the ground-towed platform. The eight receiver sensors are 0.20m diameter circular induction loops with their centers spaced 0.22m apart and covering a swath of 1.75m. The receivers are oriented horizontally (vertical axis loops) on the same plane as the 2.5m x 0.75m transmitter loop. The transmitter is powered by an external gas-powered generator and has a magnetic moment of 1350 Am².

The transmitter coil (Tx)/receiver coil (Rx) array is mounted on a fiberglass platform and towed behind a standard utility vehicle. Lines were spaced 1.5m apart to avoid data gaps. Data positioning utilized a pair of dual frequency GPS receivers recording raw data. These data were post-processed against a known base station to generate antenna locations at a nominal accuracy of 2cm. They were post-processed against each other (moving baseline correction) to calculate system orientation to a nominal accuracy of 0.1 degrees. Locations, orientations and system geometry were combined to calculate positions for each individual receiver to at least 5cm accuracy.

The console records all eight receiver values at multiple time gates at the user specified base frequency. Time gates are geometrically spaced at 0.1 ms, 0.2ms, 0.4ms and 0.8ms after the transmitter shut off. Gates continue to be recorded until the next on-time. The number of gates is therefore controlled by the choice of base frequency. The optimal base frequency was determined to be 30Hz in order to maximize the number of off-time data bins. The down-line data density is also controlled by the choice of base frequency. At typical survey speeds of 1.5m/s, a base frequency of 30Hz produces data spacing of 5.0cm.

Sensor height of the Tx/Rx array can be controlled in roughly 10cm increments. Several different platform options are available, including sled (6cm, 10cm), skis (16cm, 22cm, 27cm, 37cm, 47cm) and wheels (25cm, 28cm) depending on local ground conditions. The lowest sled option was used at both the West Jefferson and APG demonstration sites due to the flat grassy terrain. This increased the soil susceptibility response, which slightly degraded the quality of the inversion results, but it maximized the response from the small deep targets that were the primary objective of this demonstration.

5.4 DATA COLLECTION

Scale: The size, topography, background geology and a complete list of seed items for the West Jefferson and APG sites are known, and described in Section 4. Both sites were covered completely with orthogonal line directions. Target sizes range from 20mm and 37mm projectiles

at West Jefferson; 25mm to 105mm projectiles and high-explosive anti-tank (HEAT) rounds at the APG Blind Grid, and from 20mm to 40mm projectiles at the APG Small Target Grid. The APG Calibration Grid has additional items that are not used in this demonstration. This range of area size and target type is of a scale suitable to demonstrate the primary detection, classification and productivity objectives stated above.

Sample density: Cross-track spacing was determined by the receiver coil separation of 0.22m. The total swath is 1.75m, but survey lines are spaced 1.5m apart to provide sufficient overlap to avoid gaps in coverage. Down-line sample spacing is determined by a combination of base frequency and survey speed. At typical speeds (1.5m/s) and frequencies (30Hz), down-line sample spacing is expected to be approximately 5cm. After surveying in both directions, data density is approximately 180 points/m² without considering any overlap between adjacent lines. This is more than adequate to capture an entire anomaly given a system footprint of 25cm-30cm. This is the maximum resolution for surface targets. Deeper targets have larger footprints. Data are recorded continuously with internal markers indicating line number. This simplifies certain aspects of data processing, such as long wavelength drift correction that spans several lines.

5.5 VALIDATION

System performance was validated by independent third party comparison of the generated dig lists to the blind seed target locations. No additional excavation was conducted.

This page left blank intentionally.

6.0 DATA ANALYSIS PLAN

6.1 PREPROCESSING

Raw data followed three separate streams: base station GPS, platform GPS, receiver response. The base station GPS and platform GPS data were combined in differential post-processing to determine the location of the platform GPS antennae to a nominal 2cm accuracy. The two platform GPS datasets were combined in a moving baseline differential mode to determine the platform orientation. The locations, orientation and system geometry were then used to calculate the position of each receiver coil.

The raw EM data (receiver response) were recorded on the console at the chosen base frequency. All data were time-stamped to the GPS pulse per second (PPS) signal. These data were imported to a Geosoft database for processing and analysis. The differentially corrected GPS data were then imported to the same database using the PPS time-stamp.

Raw EM data were converted from units of millivolt (mV) to parts per million (ppm). A lag correction was applied based on the appropriate lag test results. Low-pass filters were applied to remove any residual high-frequency noise from the EM data. These were limited to a 5 point filter with a frequency cutoff of 6Hz. Data were then baselined using the stationary re-acquisition data at the start and end of each data file to remove low-frequency drift. Additional high-pass filters (demeaning) were applied as necessary to remove any residual effects of magnetic soil susceptibility.

6.2 TARGET SELECTION FOR DETECTION

Sensor locations were determined for each individual receiver and the full dataset was then subdivided for gridding. For the APG demonstration, nominal cell locations were provided with the objective of determining the nature of the target source (if any). Anomalies were chosen in the vicinity of each of these locations and compared to the thresholds determined from the Calibration Grid in order to declare whether or not a target had been detected.

Altitude attenuation plots for vertical and horizontal 20mmP are shown in Figure 6. The least favorable configuration at 0.60m offset should produce a target amplitude of 10ppm in the TEM-8g. This is approximately 10x the background noise level and was the nominal threshold used at APG.

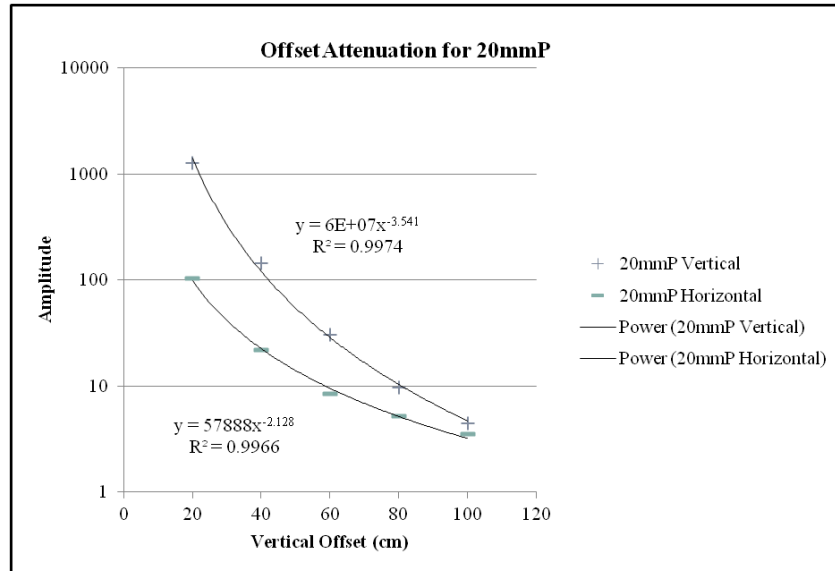


Figure 6. Signal attenuation due to altitude (offset) for a 20mm projectile. Vertical (most favorable) and horizontal (least favorable) orientations are shown. The lowest response amplitude at the maximum depth of 20x diameter (40cm depth, 60cm offset) is approximately 10mmp.

6.3 PARAMETER ESTIMATION

Data around each anomaly location were extracted from both survey directions and inverted using a dipole model to determine the target location and depth, fit coefficient, target inclination and declination, and polarizabilities (β). Each of the three polarizabilities represents the EM decay of the secondary field along one of the principle axes of the target, and is independent of target depth and orientation. Where two or more targets were clearly indicated within the same dataset, multiple dipole models were used to determine the parameters of each source. In order to perform this inversion, it was necessary to remove a certain background level from each anomalous response. This was usually the result of magnetic soil susceptibility, although baselining errors or inaccurate drift correction may also have been at fault. Where possible, a 2-dimensional (2D) map of the background soil susceptibility response was constructed for each time gate (data bin) and subtracted from the original data. When further corrections were necessary (approximately 25 anomalies), manual intervention was used to shift background levels to achieve a satisfactory inversion result.

6.4 CLASSIFICATION AND TRAINING

The data from the Calibration Grid provided a sufficient number of responses to develop an initial response library and the necessary classification rules. Polarizability data for additional unknown targets can be derived from MetalMapper libraries if necessary.

The Bin1 amplitude of the primary and secondary β , and the power of the primary decay curve represent the three-dimensional parameter space used for classification. The amplitude of the primary and secondary β are plotted against each other to determine the relative size and

dimensionality of the target (e.g., cylinder versus plate). The decay power provides an additional measure of classification related to conductivity. This has been useful in discriminating between ordnance and same-size frag, as well as between sub-classes of ordnance (e.g., 37mm projectiles with and without rotating bands). Rule-based classification routines are used within this parameter space to differentiate targets of interest from non-targets of interest.

The average and standard deviation of each parameter (Bin1 of primary β , Bin1 of secondary β , power of primary β) for each target type (e.g. 20mmP, 37mmP, 40mmP) was calculated from the Calibration Grid data. Within this three-dimensional parameter space, the “distance” of the measured response from the average value was calculated. The closest library item is the most likely source. Because these parameters all have different units, the difference in each parameter is normalized by the standard deviation to produce a single unit-less “distance” measure from the library average ($[\text{measured value} - \text{library average}]/\text{library standard deviation}$). If the response is within 4σ of the library average it is declared “Ordnance.” Those between 4σ and 6σ are declared “can’t decide.” All others are declared “Clutter.” All targets are then sorted based on their “distance” from the closest average library point to form the final dig list.

6.5 DATA PRODUCTS

The dig lists from the APG Blind Grid and Small Target Grid were submitted to ESTCP for independent third party comparison to the established seed locations. This list included the unique target identification (ID) (grid name and cell number), inversion results (Easting and Northing location, etc.) and classification declaration (ordnance, clutter, can’t decide, can’t analyze). Analysis was broken down by grid area (blind grid, small target grid), target type (e.g., 20mmP, 37mmP) and depth range (0-11x dia, 11-20x dia) in order to facilitate comparison to the project objectives. Statistics including Pd, Pcc and location error were calculated for various sub-groups and for the seed items as a whole.

This page left blank intentionally.

7.0 PERFORMANCE ASSESSMENT

In this section, the system performance is assessed for two different demonstration sites. The first is the Battelle UXO Test Grid in West Jefferson, Ohio. The second is the Standardized UXO Technology Demonstration Site at APG. The results from the Battelle UXO Test Grid are summarized as a whole and used as a baseline for establishing the performance metrics used at the APG demonstration. The APG demonstration is summarized and the final performance assessment is broken down in detail according to the objectives stated in Section 3.

7.1 WEST JEFFERSON OVERVIEW

As detailed in Section 4, the West Jefferson site was seeded with 20mm projectiles, 37mm projectiles, and 20mm-sized frag at depths between 5x and 20x the target diameter. The survey also covered targets up to 155mm projectiles, but these were not analyzed as part of this demonstration. The small target area was surveyed in orthogonal directions using a 30Hz transmitter base frequency and the sled-based platform. All targets were detected above a 10ppm threshold (10:1 signal:noise ratio) regardless of depth, yielding a Pd of 100% down to 20x diameter.

The average radial target location error was 0.06m with a standard deviation of 0.04m. The average depth error was 0.02m with a standard deviation of 0.03m. A small positioning error was detected in the data, amounting to an additional 2cm of positioning error, and producing a slightly higher standard deviation in target location error. This may also account for some of the low inversion fit coefficients.

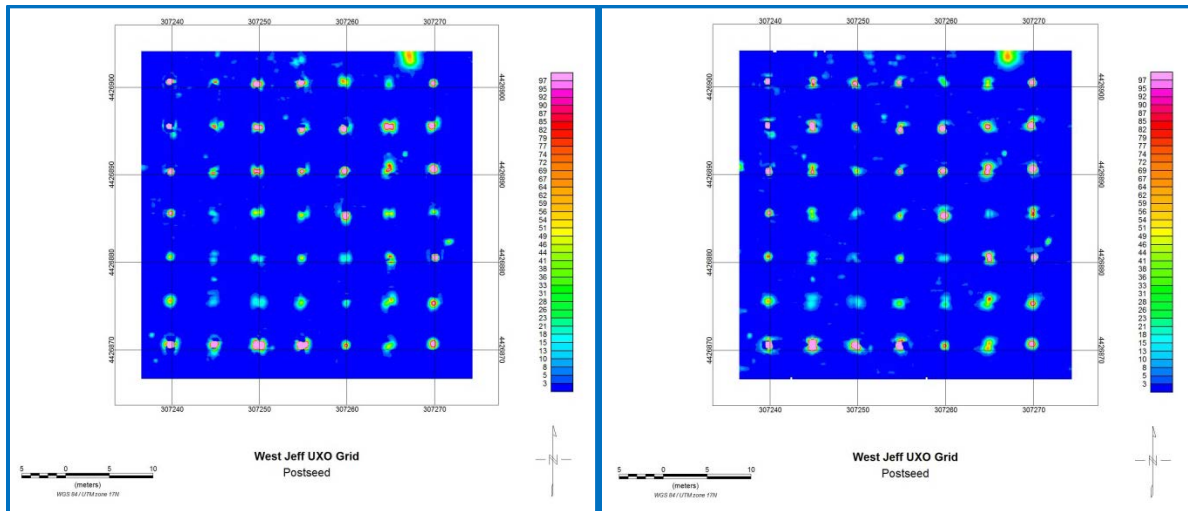


Figure 7. Thumbnail plots of the Bin2 response for the NS (left) and EW (right) survey lines at the West Jefferson Grid.

Grid lines are at 10m intervals, color scale is 0-100ppm.

Data around each target in both directions were extracted and inverted for full polarizability decays. The primary β were strong for all targets, but the quality of the secondary β depended on the signal strength. Fit coefficients ranged from 0.84 to 1.00 with an average of 0.96. Eleven targets (out of 49 total) were below the 0.96 average, and seven of those were targets (of the 11

with poor low fit coefficients) were at their maximum depth of 20x diameter. Six (6) other targets at their maximum burial depth were inverted with better than average fits.

A library of ordnance target responses was created from the inversion results. The average and standard deviation of the peak response (Bin1) of the primary β , the peak response of the secondary β , and the decay power of the primary β constitute the three axes of the classification space. The “distance” in the classification space between the response of a blind target and the average for every library target was calculated. The closest library item is the most likely source. For this demonstration, if the target distance was within 4σ of the library average then a declaration was made in favor of that target. Otherwise it was declared non-ordnance. The result of applying this rule-based classification routine to the West Jefferson dataset was a perfect receiver operating characteristics (ROC) curve.

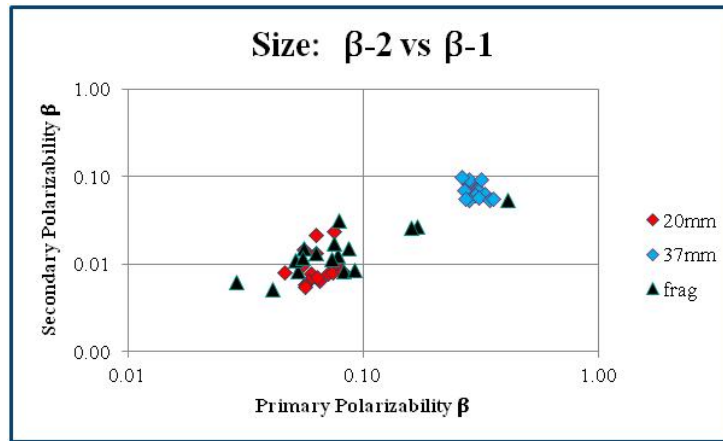


Figure 8. Plot of secondary versus primary polarizability amplitude for ground truth seeds at West Jefferson Grid.

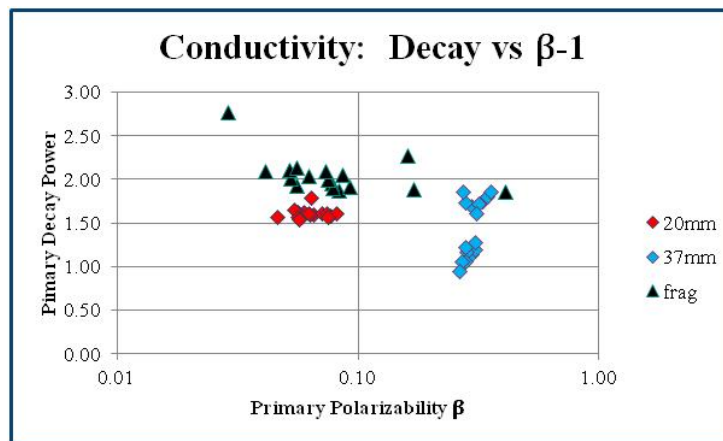


Figure 9. Plot of primary polarizability decay power versus amplitude for ground truth seeds at West Jefferson Grid.

Table 3. Averaged inversion results forming initial TEM-8g library.

UXO	$\beta 1$ (avg)	$\beta 1$ (stdev)	$\beta 2$ (avg)	$\beta 2$ (stdev)	Decay (avg)	Decay (stdev)

20mmP	0.064	0.010	0.010	0.005	1.61	0.056
37mmP (banded)	0.28	0.017	0.081	0.012	1.13	0.11
37mmP (unbanded)	0.31	0.029	0.062	0.013	1.75	0.085

avg = average stdev = standard deviation

7.2 APG OVERVIEW

As detailed in Section 4, the APG site was seeded with a range of targets from 20mm projectiles to 105mm artillery and HEAT projectiles. Four distinct grids were surveyed – two calibration grids and two blind grids. They are designated Calibration Grid, Small Calibration Grid, Blind Grid and Small Target Grid. The Small Target Grid contained 20mm, 37mm and 40mm projectiles down to 20x diameter, plus additional surface clutter of unknown size.

All four sites were surveyed in orthogonal directions using the TEM-8g with a 30Hz base frequency on the sled platform. Navigation was conducted visually with post-processed DGPS data positioning. The base station GPS was located at the civil survey monument provided (#477). Platform orientation was calculated between two GPS antenna using a moving-baseline algorithm. The nominal accuracy of the GPS antenna locations was 0.02m, and the orientation accuracy was 0.1 degree.

Data processing was limited to a low-pass filter with a 6Hz cutoff, followed by linear drift removal between periodic background points. Background readings were taken at the start and end of each data file, approximately every 30 minutes. Most background readings were taken at the clean sandy reference point provided next to the Calibration Grid. Locations for each receiver in the array were calculated using the GPS and orientation data. The processed geophysical data were then gridded with a 0.10m grid cell. The Small Target Grid required additional processing in the form of a correction for soil susceptibility. Background points were picked, gridded and the subtracted from the original data to form the final dataset for inversion.

7.2.1 Calibration Grids

In the Calibration Grid, all seed items were detected above the 10ppm threshold, including the small clutter item in Cell C3, which was approximately half the size of a 20mm projectile at 0.11m depth. The two 20mm projectiles were both detected with peak amplitudes over 100ppm. The fit coefficients were 0.91 and 0.99 for the shallow and deep targets respectively. At the other end of the spectrum, one of the larger targets (Cell E1, 105mm projectile) saturated the Bin1 data in a few sensors of the array at approximately 10,000ppm due to its shallow and vertical orientation. This is not surprising when the platform ground clearance has been optimized for 20mm projectiles at depth.

Target positioning accuracy showed a radial offset error of 0.08m with a standard deviation of 0.05m (Figure 13). A consistent 4.6cm offset in the XY locations may be the result of a documented slip in the base station GPS tripod during the survey. Calculated target depths tended to be overestimated (deeper than actual), with an average error of -0.10m and standard deviation of 0.05m. This would indicate that ground clearance of the receiver coils may be higher than expected (0.16m rather than 0.06m) due to the sled riding up on small bumps and ridges. Using this as a baseline measurement, subsequent depth-below-ground estimates are based on a 0.16m ground clearance.

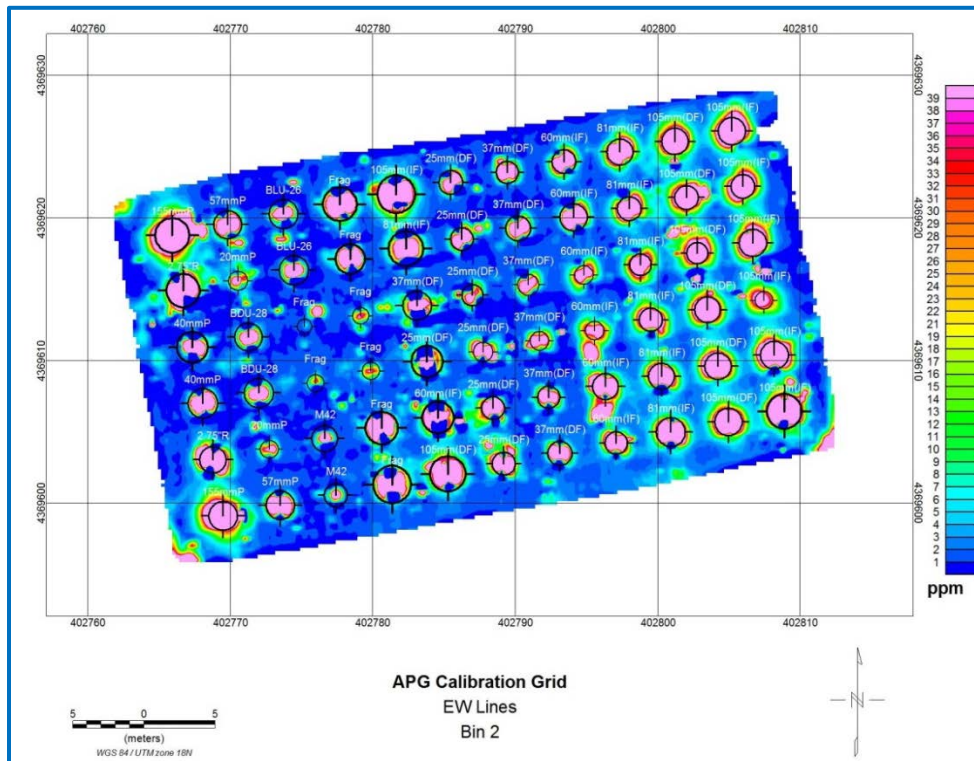


Figure 10. Plot of Bin2 response at APG Calibration Grid.

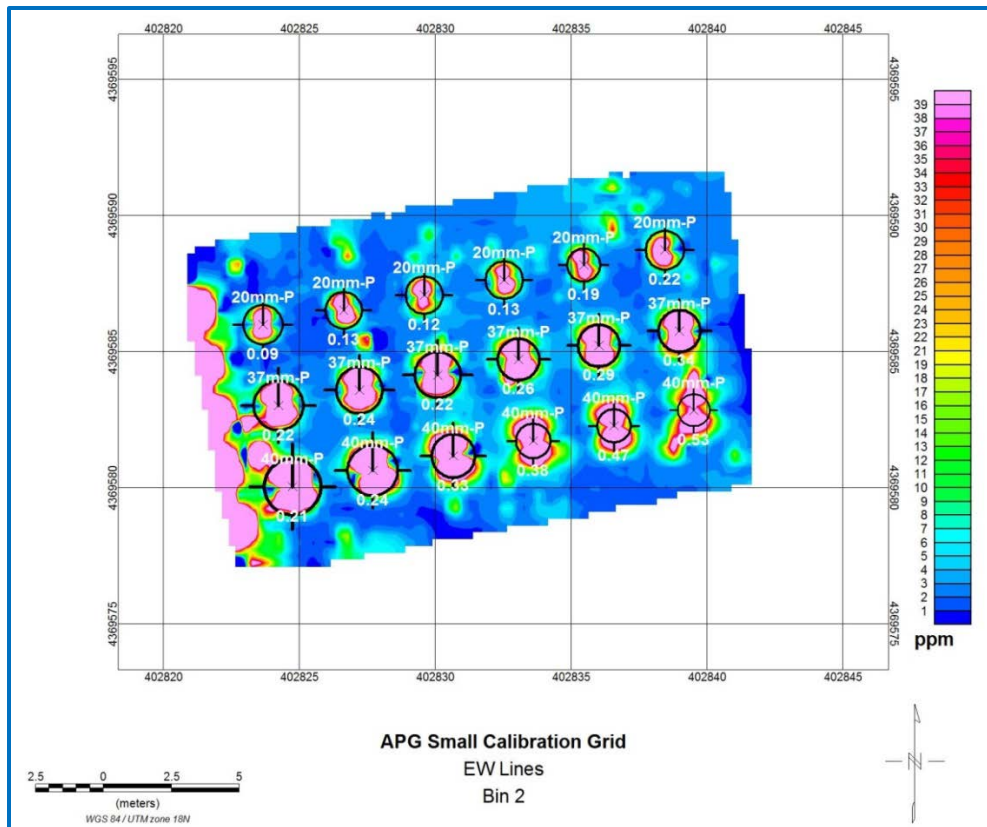


Figure 11. Plot of Bin2 response at APG Calibration Grid.

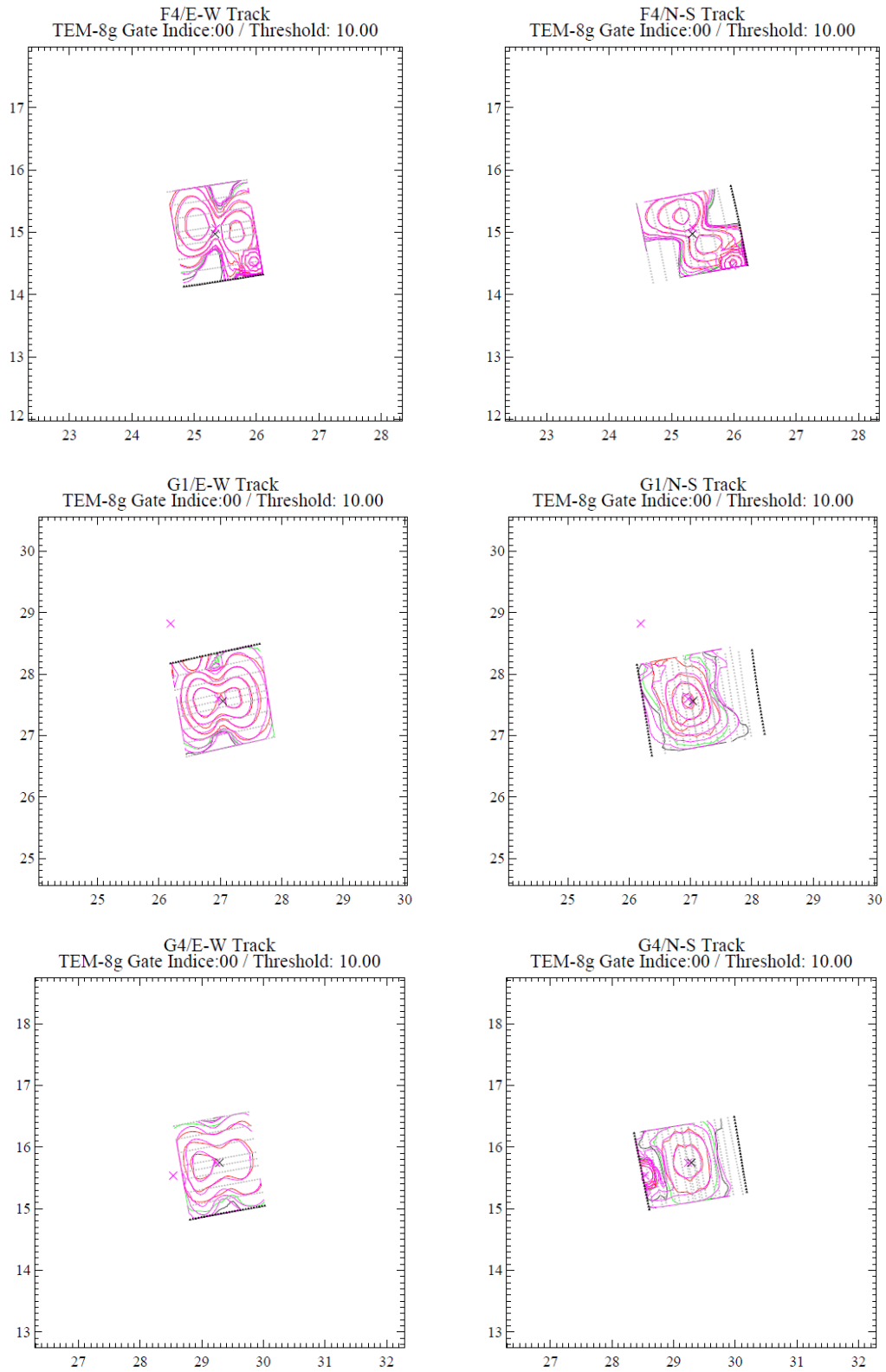


Figure 12: Overlapping contours of measured and modeled (from inverted target) results of 2-dipole models for anomalies in Calibration Grid Cells F4 (25mm), G1 (37mm) and G4 (37mm).

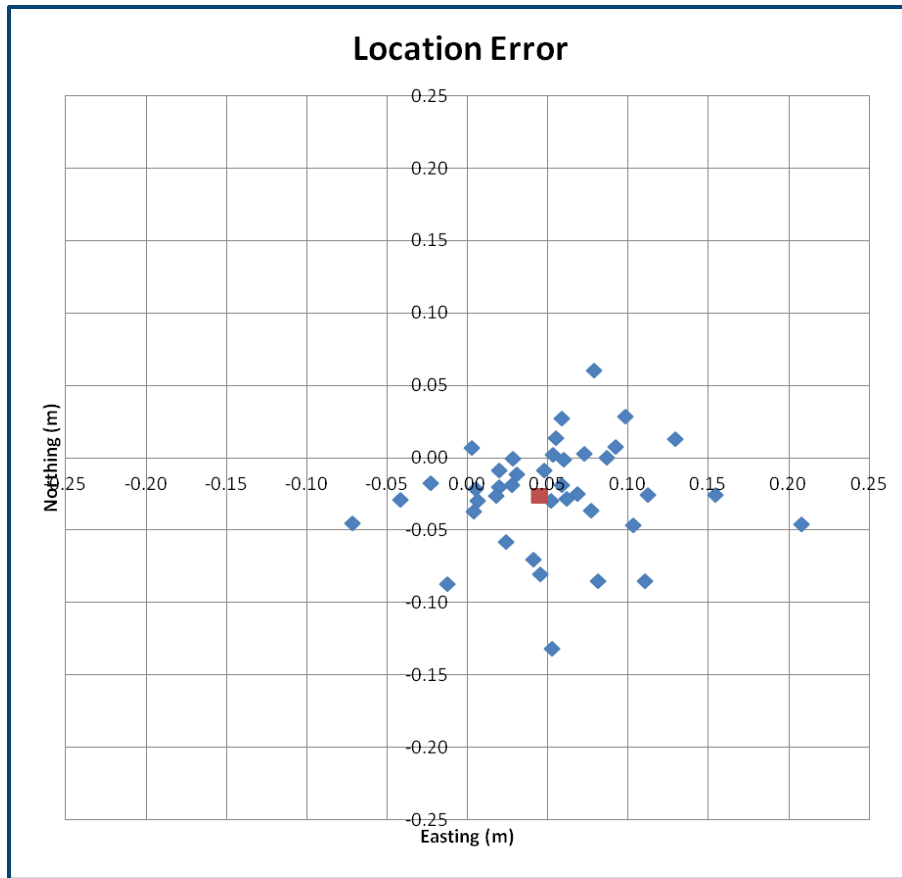


Figure 13. Calibration Grid location error plot.

The average offset is shown in red. The standard deviation is 0.05m

The inversion results from the Calibration Grid and the Small Target Calibration Grid were added to those from the West Jefferson dataset to produce a library of targets that were used to classify the results of the APG Blind Grid and Small Target Grid (Figure 14 and Figure 15). The 25mm targets showed a wide scatter in the parameter space plots, but do not appear to form separate sub-groups. The 20mm targets also show a wide scatter, but in this case they appear to form at least two or possibly three separate groups. These may be legitimate variants, or the spread may be the result of weak SNR because these targets are an order of magnitude smaller in both primary and secondary β than the 37mm or 25mm targets. When compared to the inversion results from the Blind Grid and Small Target Grid, the West Jefferson calibration items were clearly not of the same variety of those used at APG and so this sub-group was dropped from the library for the purposes of classifying the APG Small Target Grid data (see Figure 20).

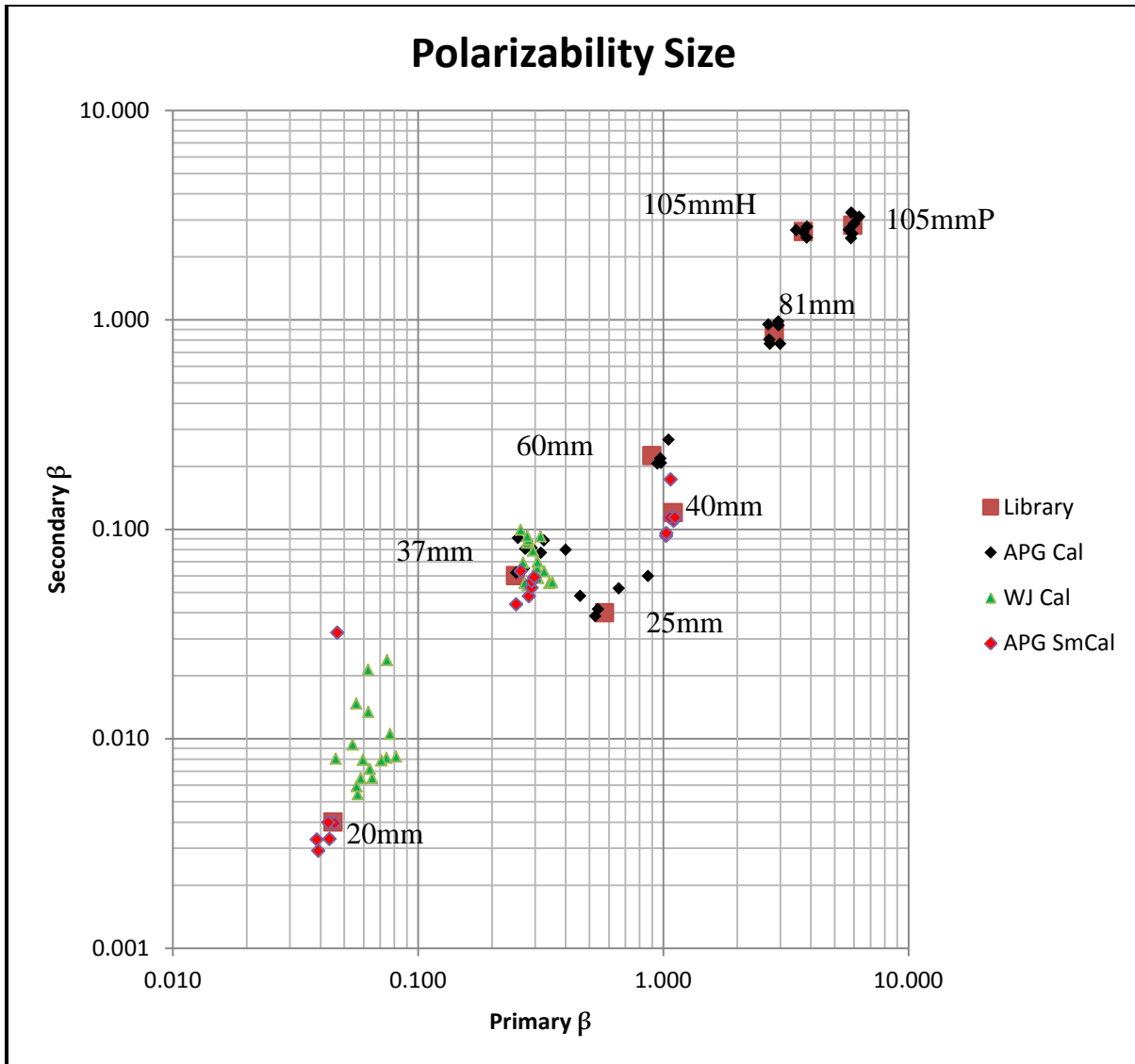


Figure 14. Plot of secondary versus primary polarizability amplitude for calibration items. Points include individual results from the West Jefferson and APG Calibration grids, as well as the final Library reference point used for classification of the APG grids.

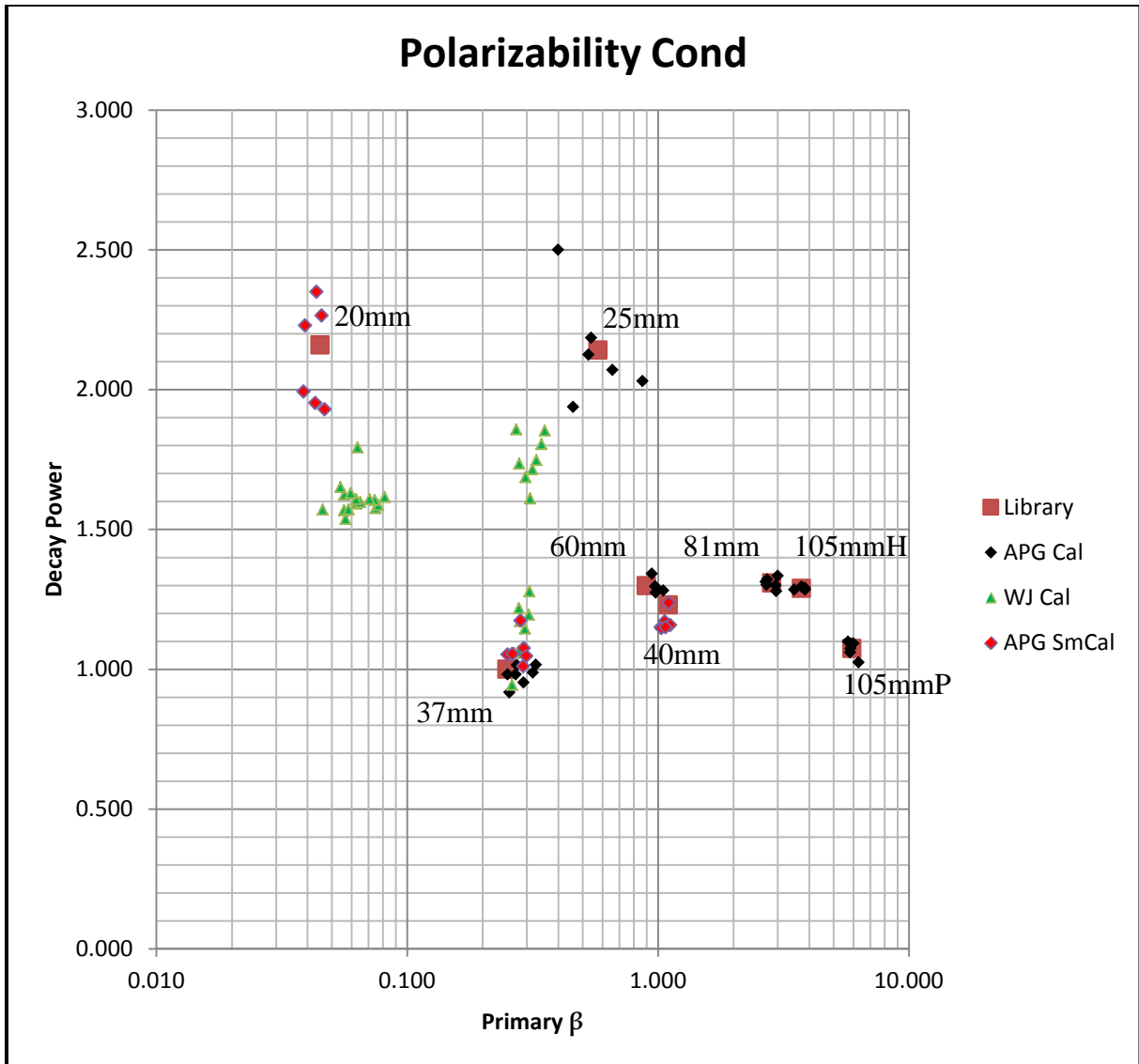


Figure 15. Plot of primary polarizability decay power versus amplitude for calibration items.

Points include individual results from the West Jefferson and APG Calibration grids, as well as the final Library reference point used for classification of the APG grids.

7.2.2 Blind Grid

In the Blind Grid, all targets above the 10ppm threshold were selected. Those cells below the threshold were declared blank. Targets were inverted and classified according to the procedure detailed above. This list was submitted to ESTCP for analysis.

Plots of the polarizability parameter space are presented below. This illustrates the clustering of the Blind Grid inversion results about the Calibration Grid library results (Figure 17).

Results of the ground truth analysis were presented in several formats. The first is a ROC curve (Figure 18). This shows the probability of detecting a true target (ordnance) against the probability of detecting a false target (clutter) when using a prioritized dig list. Two lines are plotted. The orange line is the ROC curve if the dig list is sorted based on response amplitude only. The blue line is for the dig list based on the discrimination results. The difference between the two illustrates the amount of clutter on the site.

Black horizontal lines are used to illustrate the performance at two specified points: at the response stage threshold (orange star), representing the point below which targets are not considered detectable; and at the discrimination stage threshold (green star), defining the subset of targets the demonstrator would recommend digging based on discrimination. The response stage threshold is at an amplitude of 10ppm, which is roughly 10x the noise floor of the sensor system.

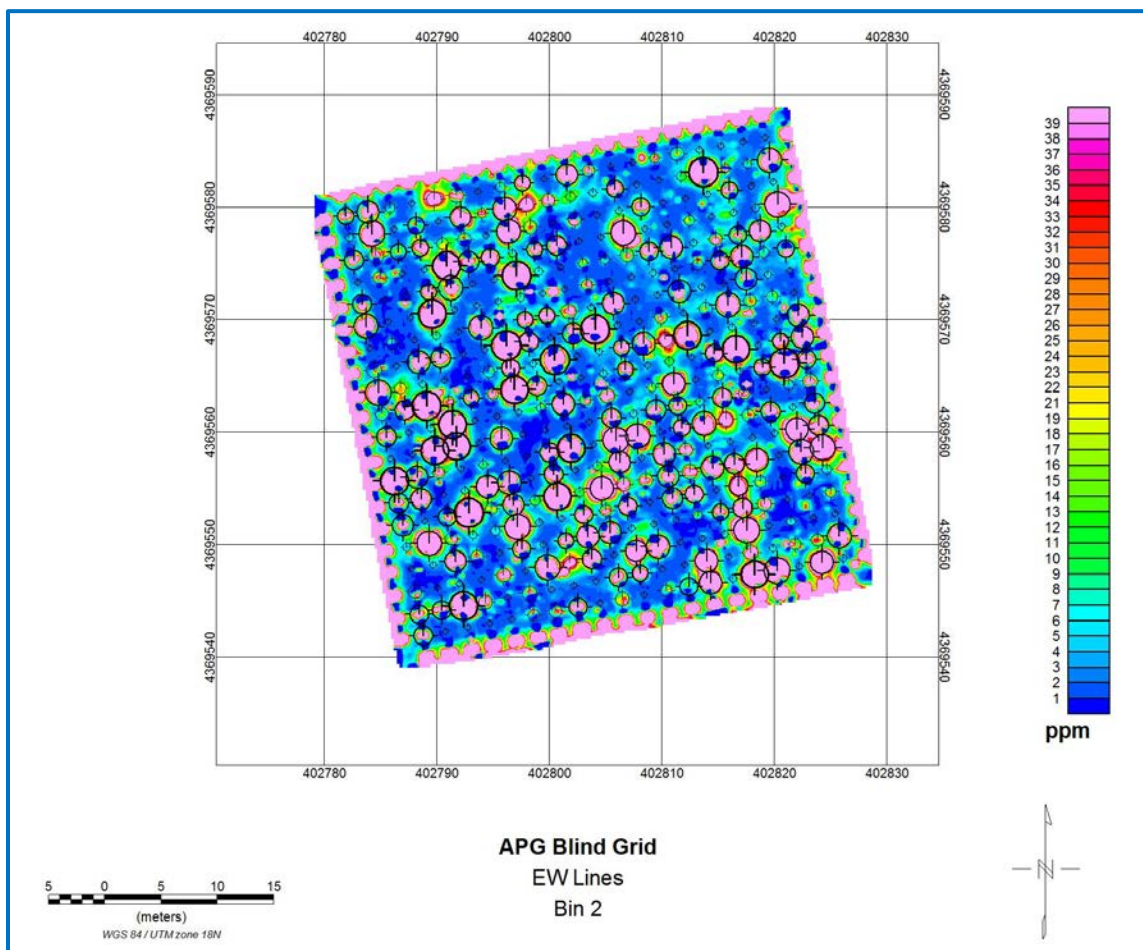


Figure 16. Plot of Bin2 response at APG Calibration Grid.

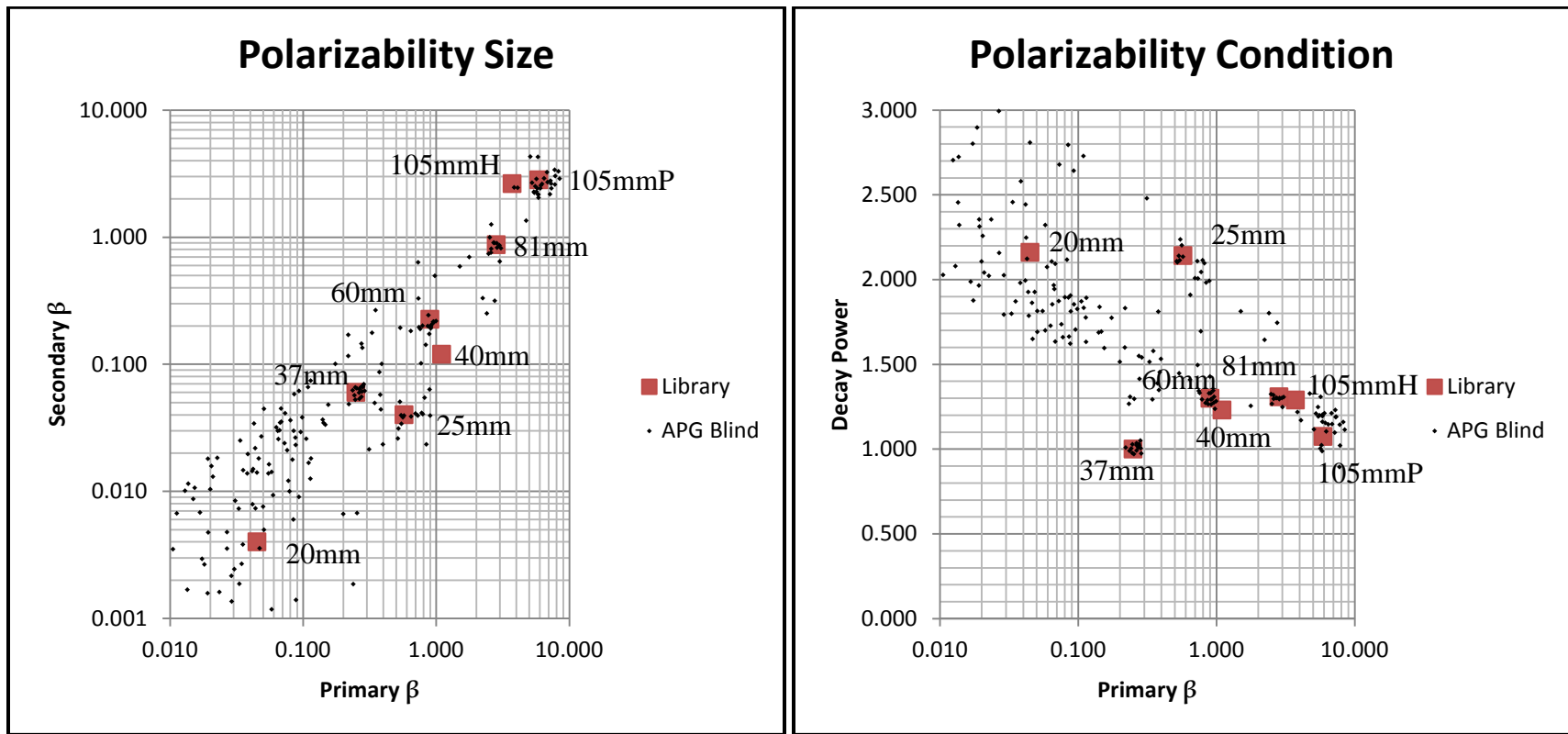


Figure 17. (a-left) Plot of secondary versus primary polarizability amplitude and (b-right) primary polarizability decay power versus amplitude.

Points include the Library reference points and all detected targets from the APG Blind Grid.

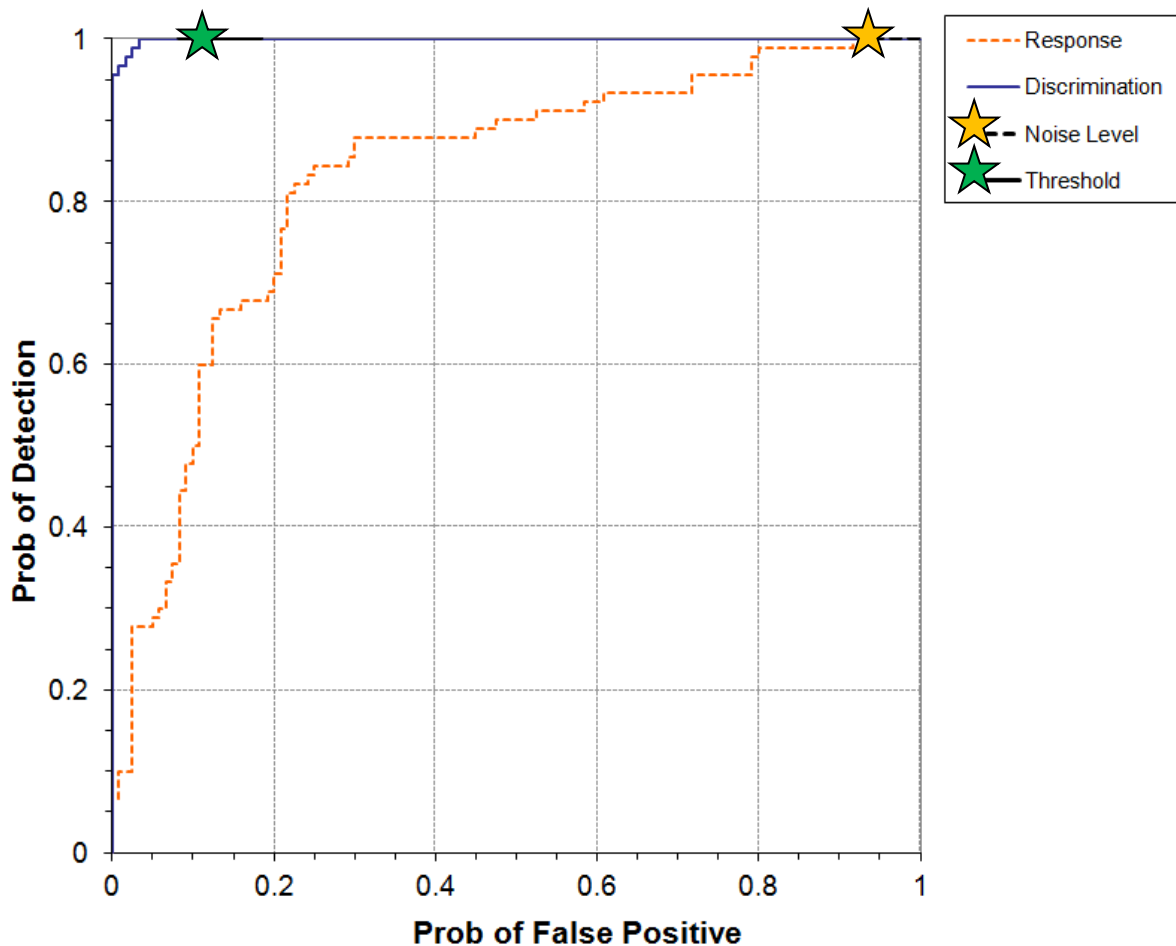


Figure 18. ROC curve for TEM-8g at Blind Grid.

Probability of detection for response and discrimination stages versus their respective probability of false positive.

The results presented here illustrate near perfect discrimination in a lightly cluttered environment. In retrospect, the threshold limit was set slightly higher than necessary, allowing some clutter items into the classified dig list.

7.2.3 Small Target Grid

In the Small Target Grid, all targets above the 10ppm threshold were selected. Those cells below the threshold were declared blank. Targets were inverted and classified according to the procedure detailed above. This list was submitted to ESTCP for analysis. A second list based on SAIC's shape/scale classification system was also submitted for comparison. Both lists were based on the same polarizability results, but used different classification procedures.

The differences between the two dig lists were relatively minor. Both lists detected all targets above the noise threshold. In classification, both lists used a threshold below the 100% Pd level. The Battelle list used a slightly lower discrimination threshold than SAIC. This captured more of

the ordnance and resulted in slightly better Pdisc statistics at the cost of higher Pcc (reported statistics are based on all digs above the discrimination threshold).

Plots of the polarizability parameter space are presented in Figure 20. This illustrates the clustering of the Small Target Grid inversion results about the Library reference points. Classification based on these results produced the ROC curves presented in Figure 21 and Figure 22.

Scoring results were divided into capped and uncapped subgroups. The uncapped group replicates the standard seeding procedure used throughout the APG demonstration facility where the area around the target has been cleared of all (most) metallic debris. The capped group has deliberate clutter items placed directly on top of the target location in order to mask the signature and make classification more difficult. This is closer to what may be presumed to be found in a live-site situation rather than a typical controlled test plot. The combination of small targets, increased burial depth, native clutter and high levels of soil susceptibility, together represent a worst-case scenario for APG demonstration purposes.

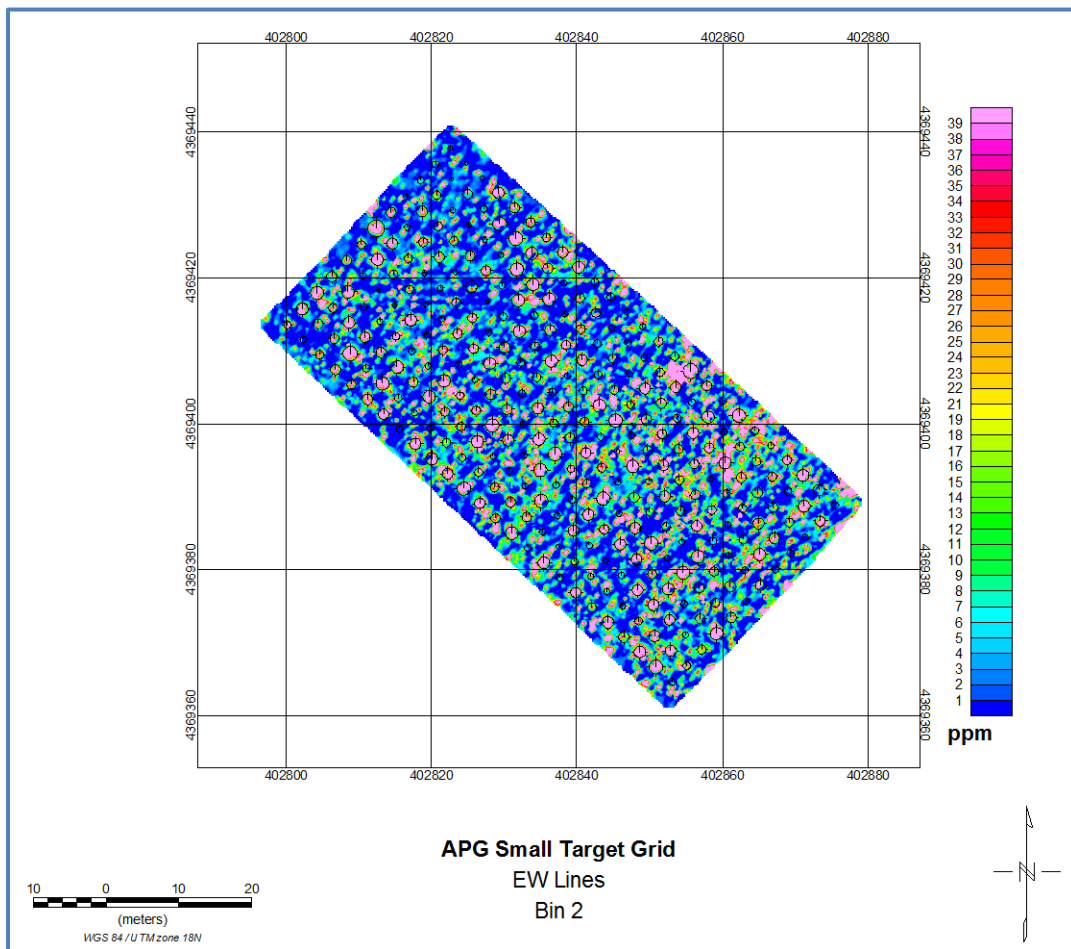


Figure 19. Plot of Bin2 response at APG Calibration Grid after removal of background susceptibility.

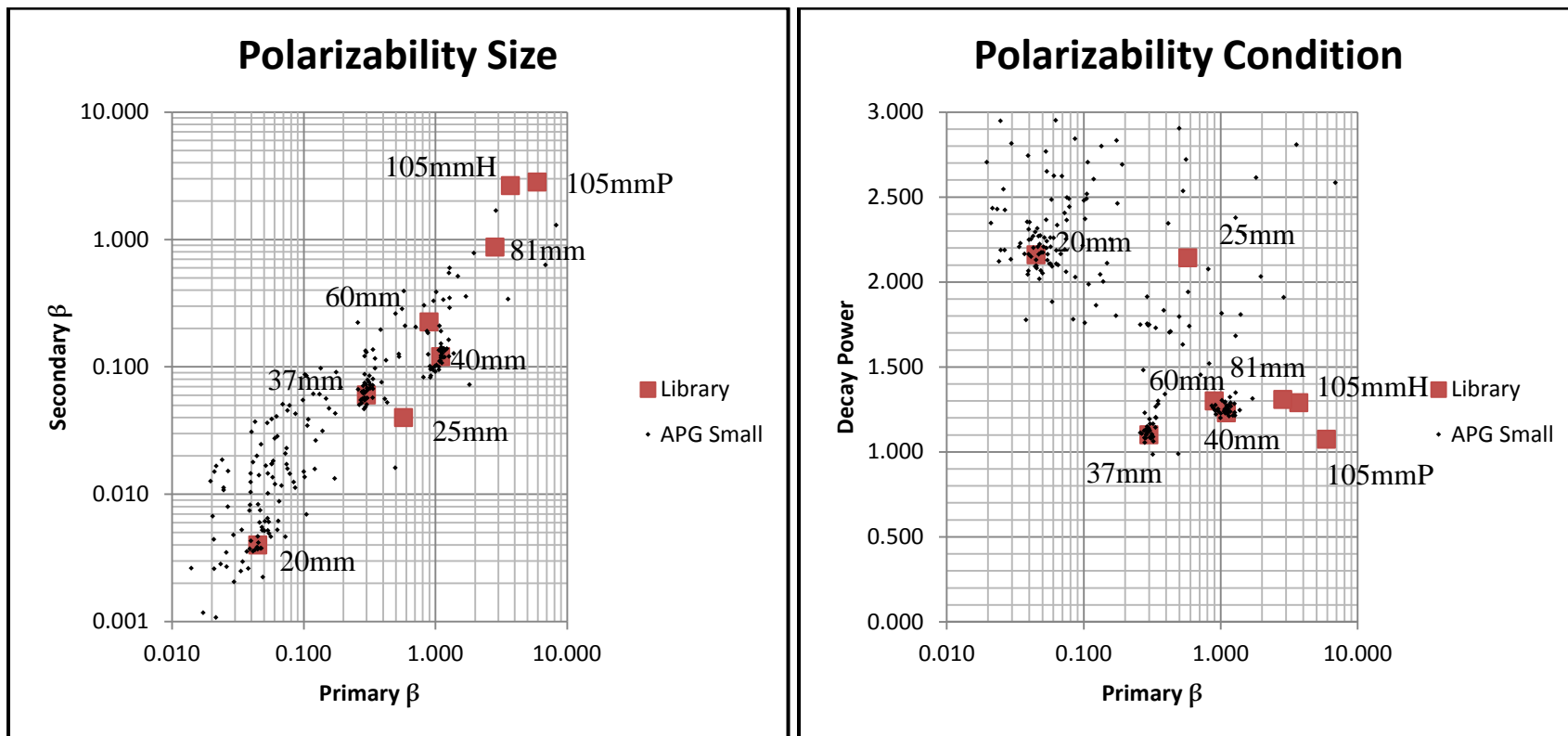


Figure 20. (a-left) Plot of secondary versus primary polarizability amplitude and (b-right) primary polarizability decay power versus amplitude.

Points include the Library reference points and all detected targets from the APG Small Target Grid. Note that the variant of 20mm projectiles used at the West Jefferson test grid are not represented in this dataset.

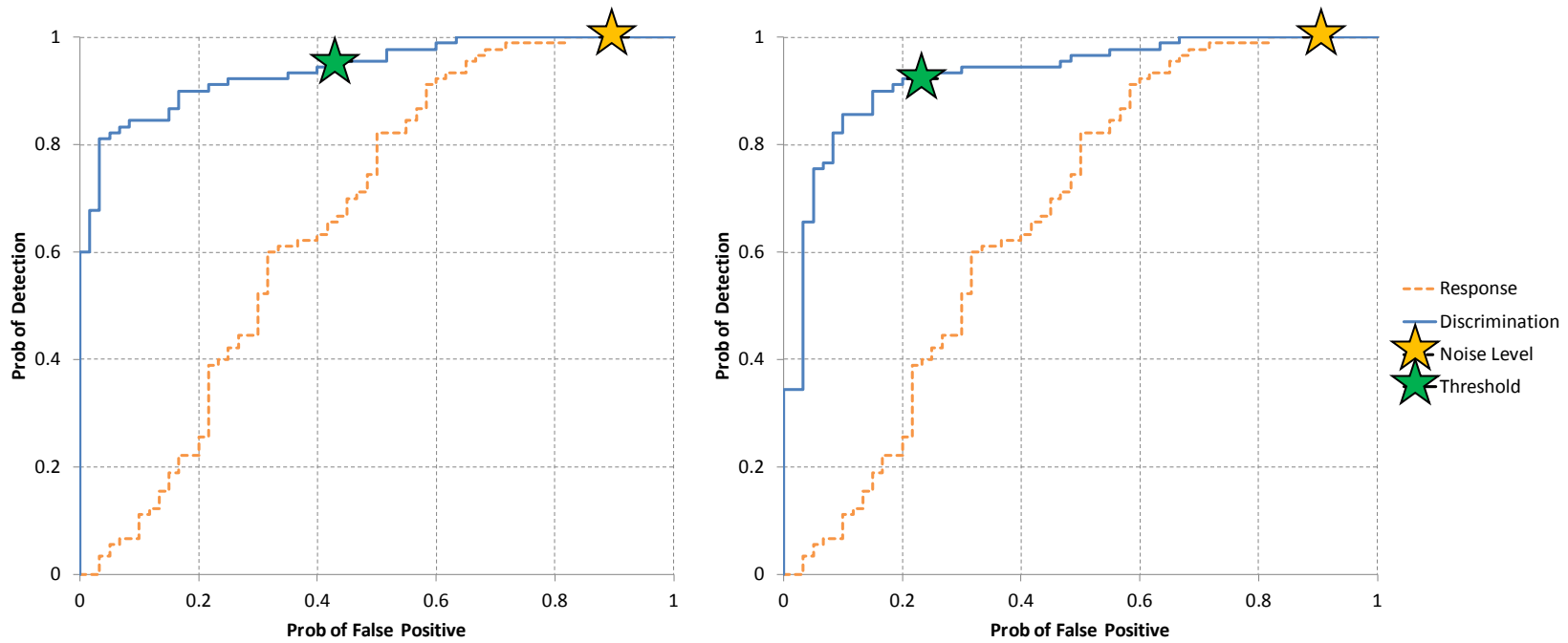


Figure 21. (a-left) ROC curve from Battelle list, Small Target Grid, capped cells, all ordnance types, depths to 20x diameter. (b-right) ROC curve from SAIC list, Small Target Grid, capped cells, all ordnance types, depths to 20x diameter.

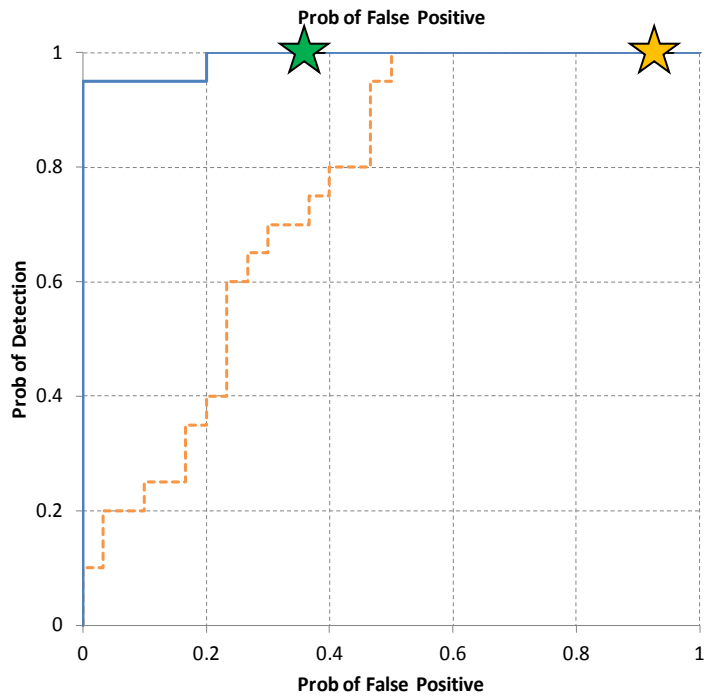
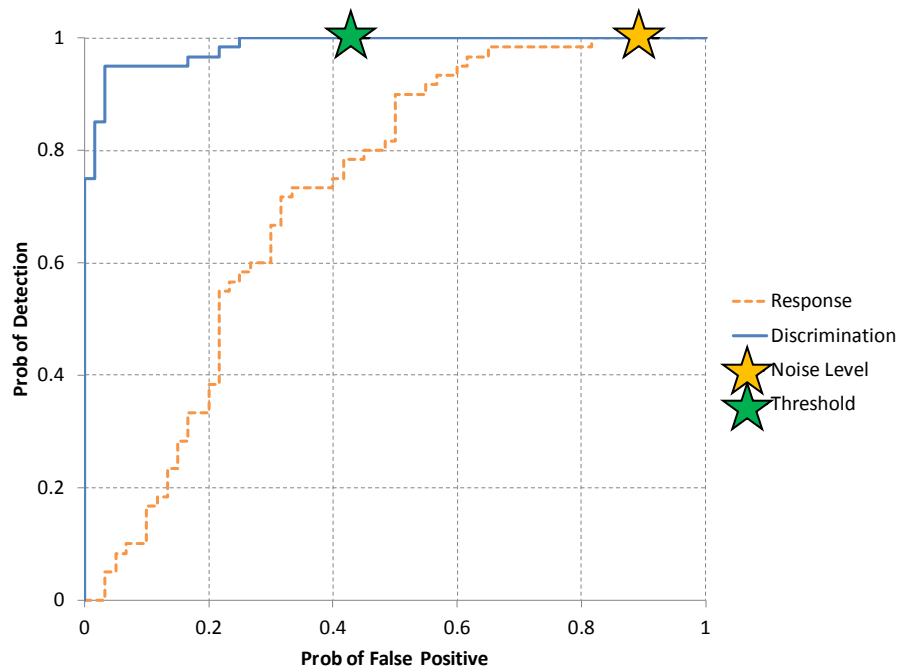
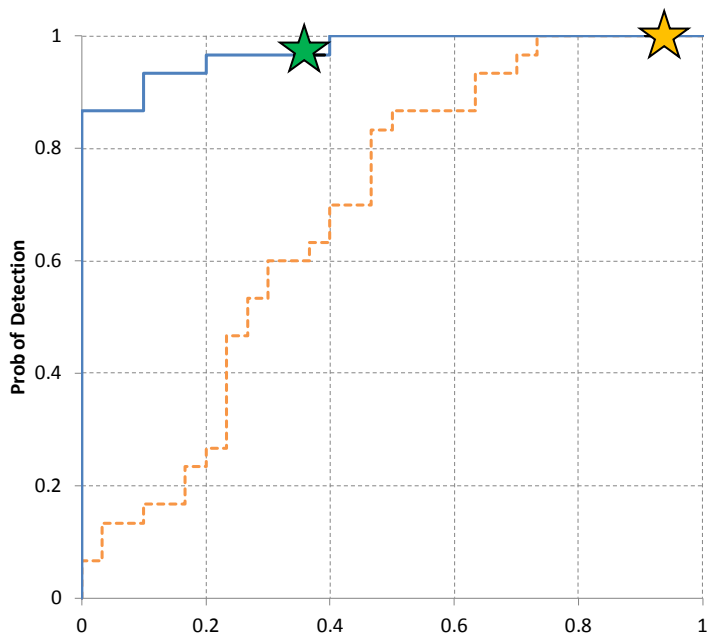


Figure 22. (a-top left) ROC curve from Battelle list, Small Target Grid, uncapped cells, all ordnance types, depths to 20x diameter. (b-top right) ROC curve from Battelle list, Small Target Grid, capped cells, 37mm and 40mm ordnance types, depths to 20x diameter. (c-bottom left) ROC curve from Battelle list, Small Target Grid, uncapped, 37mm and 40mm ordnance types, depths to 20x diameter.

7.2.4 Analysis

Data collection at the APG site was relatively simple. The logistics and terrain were ideal. The resulting data were relatively free of instrument noise. The Small Target grid had considerable background geophysical noise from pre-existing clutter and soil susceptibility.

Data processing followed a routine comparable to that of an array of EM61s. A small low-pass filter was followed by baseline leveling between background points collected over the clean sand pit at the north end of the area. The data from Small Target grid required additional background removal of the soil susceptibility before inversion.

Inversion was run mostly in an automated fashion on bi-direction (orthogonal) survey data, which included up to four-dipole models for each cell. Some manual intervention was required to obtain acceptable inversion results on 25 cells, of which 7 remained unacceptable.

Classification was based on the inversion results using two different techniques. The SAIC method used the amplitude and shape of the primary polarizability curve only to match library points. The Battelle method included the secondary curves. Discrimination thresholds were established independently for both approaches based on the last reliable ordnance declaration. The two results are very similar but the Battelle list used a lower discrimination threshold that skews some of the numbers to higher P_{disc} and lower false positive (FP) rejection. Except where specified, this report considers the Battelle results in the analysis. The Response Stage of the dig list is based entirely on response amplitude. As such, it is only an intermediate product and analysis will focus on the Discrimination Stage results.

The scores for the Blind Grid demonstrate near perfect detection, classification and clutter rejection capabilities for targets between 25mm and 105mm sizes at standard depths. The results appear to be better for small targets rather than large ones. This is due to the fact that the system operating parameters were optimized for 20mm targets at depth. Larger targets, particularly the 105mm HEAT and projectiles, and the shallow, vertically-oriented 81mm mortars would occasionally saturate the response making the inversion and classification inaccurate. Given the size and depth of the targets in this grid, the Blind Grid results are the ones that should be used when comparing this system's performance to that of other dynamic discrimination instruments.

The Small Target grid results were excellent, but require more detailed analysis. The "capped" results represent the worst case scenario. In this case, the "elbow" of the ROC curve is at approximately $P_{disc}=85\%$ and $FP=15\%$. The list eventually reached $P_d=100\%$, but the discrimination threshold was set higher at $P_{disc}=96\%$ and $FP=48\%$. The "uncapped" results were slightly better with an elbow at $P_{disc}=90\%$ and $FP=10\%$ and a threshold point at $P_{disc}=97\%$ and $FP=39\%$. Therefore, the additional clutter cap had no impact on the P_{disc} but increase the FP by approximately 10%. This would imply that the cap disguised the clutter response, making it more likely to be declared ordnance, presumably by adding ambiguity to the inversion results.

The Blind Grid and the Small Target grid results can be compared by looking at the respective ROC curves. The ROC curve for the uncapped cells with 37mm and 40mm ordnance types is comparable to the conditions in the Blind Grid. The ordnance size at least partially overlaps and

there is no additional clutter cap directly over the target. The primary difference here is that the burial depths extend to 20x diameter, although the change in background conditions (soil susceptibility and native clutter) is also a factor. The change between Figure 18 and Figure 22c therefore demonstrates the reduction in classification capabilities (Pd detection remains at 100%) due to depth for this target size. In this case, the Pdisc and FP rejection (1-FP) numbers drop from 1.00/0.87 to 1.00/0.65 at the discrimination threshold point. This would indicate that roughly 20% more clutter items would be dug by doubling the detection depth for targets in the 37mm to 40mm size range.

The choice of library reference points necessarily has a significant impact on the classification results. The 40mm library was based entirely on the results from the APG Calibration Grid. The 37mm and 20mm library included results from the West Jefferson Test Grid. The 40mm targets showed good SNR and a tight clustering about the library point. The 20mm targets showed an order of magnitude weaker response in the primary and secondary polarizabilities. This resulted in generally poorer inversion fits, and a correspondingly broader target scatter. There also appears to be a significant difference in response between the 20mm ordnance used at West Jefferson and those at APG, even though both appear to have come from a common source (West Jefferson seed targets were all labeled as Aberdeen Test Center). None of the Small Target Grid inversion results matched the calibration measurements from West Jefferson, so this reference point was dropped from the library for the purposes of classification of APG data.

The 37mm targets were known to have at least two different variants (with and without rotating band). These were represented in the West Jefferson library measurements but were not observed in the APG Calibration grid. However, there were sufficient responses in the Small Target Grid that matched the second variant that both variants were included in the classification process. If the Small Target Grid seed items match the Calibration items (one variant only), this may account for some of the FP responses observed in the final scoring. A comparison of the ROC curves with and without the 20mm targets (Figure 22a and Figure 22c) indicates most of the FPs result from the classification of 20mm targets. With so few FPs in the 37mm category using two variants of 37mm, this would indicate that both variants of 37mm are likely present in the Small Target Grid. In an active field project, the presence or absence of the second variant would be determined early in the excavation process and the dig list would be modified accordingly in order to maximize efficiency.

The tabulated results show that all of the 40mm and 37mm targets at all depths both with and without caps were detected above the discrimination threshold. The 20mm targets were all detected above the noise threshold, but not above the discrimination threshold. A lower threshold would improve the Pd results at the expense of the FPs. At the current discrimination threshold, the uncapped seeds were all detected down to 11x diameter, but the deeper targets were not. The clutter cap made discrimination more difficult even for the more shallow targets. It is interesting to note that the capped targets at 20x depth showed a higher Pdisc than the uncapped targets at the same depth. This is presumably because the local site variations in soil susceptibility and native clutter have a larger impact on the results than the emplaced clutter cap.

7.2.5 Conclusions

All targets in the Blind Grid and Small Target Grid were detected in the Response Stage, resulting in Pd of 1.00. In the Discrimination Stage, bi-directional (orthogonal) survey data were required for inversion. All targets in the Blind Grid and all 37mm and 40mm targets in the Small Target Grid were detected at all depths, resulting in a Pdisc of 1.00. The 20mm targets had Pdisc reduced to 0.87/0.90 (capped/uncapped), primarily at the greater depths. Classification of clutter (Pcc) was slightly lower than the corresponding Pdisc, reflecting a cautious approach to declarations. Pcc was 0.87 in the Blind Grid, and 0.52/0.61 (capped/uncapped) in the Small Target Grid. This last metric was the only one that came close to falling below the design expectations. All metrics surpassed those of the existing technology standard (EM61 array).

In projecting these results to other sites, terrain and obstacles may require additional ground clearance of the instrument. Based on the amplitude attenuation for a 20mm target in its least favorable orientation, a 10ppm noise threshold falls at a 60cm offset. The sled configuration used at APG had a ground clearance of 6cm. Higher ground clearance options are available but will necessarily result in poorer performance at extreme depths. For example, with a Discrimination Stage Pdisc of 0.87 for a 20mmP at a 20x burial depth (offset of 46cm), one would expect the same Pdisc at the same overall offset, such as 11x burial depth plus 23cm ground clearance. Similarly, larger targets could get the same 100% Pdisc at 11x burial depth with much greater ground clearance if necessary.

In conclusion, this project met all of the original expectations for small target detection at depth, and greatly exceeded expectations in terms of discrimination and classification. Originally intended purely as a detection tool and replacement for the standard EM-61 array, this system has demonstrated superior depth detection and comparable discrimination capabilities to other dynamic classification tools as demonstrated at the APG site.

8.0 COST ASSESSMENT

The expected operational costs for this technology have been developed based on the actual costs incurred after adjustment for circumstances unique to this demonstration. The resulting cost model is broken out into the follow categories: instrument costs, mobilization, equipment setup and calibration, survey costs per acre, demobilization, data analysis. Cost tracking elements for each of these are shown in Table 4.

Table 4. Cost model metrics.

Cost Element	Data to be Tracked
Instrument costs	Engineering estimates based on current build
Mobilization	Actual demonstration costs
Equipment setup/cal	Hours and personnel required
Survey costs	Hours and personnel required for each configuration demonstration, reduced to a cost per hectare
Data processing	Hours and personnel required for each configuration, reduced to a cost per hectare

8.1 COST MODEL

Instrument costs for this demonstration were largely covered by using existing electronics. This includes the controller and data logging console, multiple GPS units, navigation system and power supply. New equipment included the transmitter and receiver coils, cables and connectors. A variety of tow platforms were also constructed. In total, five different platforms options were constructed including a fiberglass version with options for wheels (2) or skis (2), and a sled (1). The tow vehicle was rented from a local equipment supply firm. The console was designed for airborne survey applications and has considerable redundancy. The cost to replicate the total system including the airborne data console is given below. In a production setting, the console configuration could be much simpler and less expensive.

Total prototype equipment cost: \$180k

Mobilization costs included one day of packing, one day of driving, one day return, one day unpacking for two people each day. Travel costs were at government per diem rates. Actual costs will vary depending on the mileage, distance and personnel involved.

Mob/demob costs: \$12k

Calibration consisted of warming up the instrument and taking the prescribed quality control (QC) measurements. This requires approximately 1 hour. Equipment setup, consisting of unpacking and assembling the system requires approximately 3 hours. Costs are calculated for a total of 4 hours.

Setup and calibration costs: \$1.8k

Survey costs are based on a 3 person team. It required 1 hour (55-60 minutes) to complete a single full coverage pass over the Small Target Grid (0.28 ha) for each configuration tested. This

included relocating the array to the quiet calibration point at the other end of the site every 30 minutes (start, middle and end of a pass). Two orthogonal passes were required to provide sufficient data to perform inversion. Production rates are therefore 0.14 ha/hour. Costs include labor, travel and equipment rental, and totaled \$450 per hour.

Survey costs: \$3.2k/ha

Actual data processing costs for the Blind Grid (0.16ha) and Small Target Grid (0.28ha) totaled \$15k for this project, including one processing geophysicist and one inversion specialist. This covers three passes over each grid using different ground-clearance options, although only one configuration was used in the final analysis. This amount does not include the cost to develop the basic processing and inversion routines, but it does include time to develop new processing routines to handle the high magnetic susceptibility in the soils at the Small Target Grid and to develop classification routines from multi-dipole inversion results. If the project costs are assumed to be related entirely to a single pass over the Small Target Grid and the Blind Grid, the cost is approximately \$34k/ha. In a production setting, estimated processing costs would be much lower.

Estimated production processing costs: \$3.4k/ha

8.2 COST DRIVERS

Cost drivers are relatively simple. Deployment issues (terrain and vegetation) may impact the utility of the collected data by limiting coverage or ground clearance; but they have only minor impact on the costs. Mobilization and setup are no more difficult or expensive than an array of standard EM-61 sensors. Survey costs may initially appear to be high due to the requirement for bi-directional surveying, but the wide swath width and relatively high survey speeds more than compensate. Survey costs should therefore be twice those of a detection-only survey with an EM-61 array, but half that of a dynamic survey with a classification instrument such as MetalMapper. Initial processing costs should also be comparable to an array of EM-61s. Inversion and classification costs should be slightly less than those of a dynamic MetalMapper due to the simpler data presentation requirements.

A comparison of productivity statistics for various geophysical systems is provided in Table 5. These are estimates only, but demonstrate that the TEM-8g has approximately half the productivity of an EM-61 array, but twice that of dynamic classification systems. The “time on grid” number is based on the EM-61 array as the industry standard instrument. In terms of cost drivers, the additional time on grid relative to the EM-61 array must be offset by the detection depth and classification capabilities of the TEM-8g. The data density numbers are significant in that they illustrate the resolution of the various systems and reflect their ability to detect and isolate small ordnance types and/or closely spaced debris.

Table 5. Productivity statistics for a variety of detection and classification instruments.

Instrument	EM-61- array	TEMTADS 2x2	ALLTEM	Dynamic MM	TEM-8g
Line Spacing (m)	2.0	0.75	0.5	0.75	1.5
Speed (m/s)	1.0	0.5	1.0	0.5	1.5
# Passes	1	1	1	1	2
Productivity (m ² /s)	2.0	0.37	0.50	0.37	1.1
Relative Time on Grid	1x	5.5x	4x	5.5x	2x
Sample Rate (Hz)	10	10	10	10	30
Data Spacing (m)	0.75	0.5	0.5	0.75	0.22
Data Density (1/m ²)	13.3	40.0	20.0	26.6	180

8.3 COST BENEFITS

The costs benefits of this technology fall into two categories. The first is improved depth detection for small targets when compared to the existing technology (EM-61 array). This system effectively doubles the reliable detection depth, thereby halving the geophysical survey costs required to clear an area of small targets down to a reasonable depth.

The second benefit is the capability of ordnance classification from a dynamic platform. The reliability of the inversion results from the TEM-8g greatly surpasses that of the traditional technology it is designed to replace. Other “next-generation” dynamic systems also offer this capability, some with greater confidence. However, none have demonstrated the same reliability with regard to small targets, or the rapid productivity (wide swath width), or the “20x” depth capability of the TEM-8g.

At the very least, this system can double the depth of investigation, improve detection resolution and reduce the number of cued investigations required during a standard two-stage geophysical program. At best, it may replace the need for cued investigations at many sites.

This page left blank intentionally.

9.0 IMPLEMENTATION ISSUES

The current prototype system is immediately available for implementation on small scale projects. Larger projects will require a more rugged platform to handle more difficult terrains for long periods. A commercial version of the system would require the design and manufacture of a simplified controlling console (the current console is primarily designed for airborne operations).

All data processing is currently handled within Geosoft, but a production version of the inversion software is required for routine work. Basic geophysical knowledge is required to operate and process the data. Any geophysicist familiar with the workflow for an EM-61 array can handle the basic processing. Analysis of the inversion results has largely been automated, but additional experience is required to optimize various parameters.

End users will be reluctant to accept results from this (or any) new technology on the basis of a single controlled-site demonstration. Additional demonstrations at live-sites will be required to mitigate those concerns. No potential regulatory restrictions have been identified for this technology.

This page left blank intentionally.

10.0 REFERENCES

- Asch, T.J., 2011. ALLTEM Multi-Axis Electromagnetic Induction System Demonstrations and Validation, Final Report ESTCP MR0809.
- Aberdeen Test Center (ATC), 2007. Final Report for the Evaluation of Unexploded Ordnance Detection Technology at the Standardized UXO Test Sites Aberdeen and Yuma Proving Grounds, Final Report ESTCP MM1300.
- Billings, S., 2011. Next Generation Data Collection System for One-Pass Detection and Discrimination, Final Report ESTCP MM0908.
- Harbaugh, G.R., Steinhurst, D.A., and Khadr, N., 2008. ESTCP UXO Discrimination Study MTADS Demonstration at Camp Sibert Magnetometer/ EM61 MkII/ GEM-3 Arrays, Final Report ESTCP MM0533.
- Nelson, H.H., Bell, T., Kingdon, J., Khadr, N., and Steinhurst, D.A., 2008. EM61-mk2 Response of Standard Munitions Items, NRL/MR/6110-08-9155.
- Nelson, H.H., Kaye, K., and Andrews, A., 2009. Geophysical System Verification (GSV): A Physics-Based Alternative to Geophysical Prove-Outs for Munitions Response, ESTCP Final Report.
- Naval Research Laboratory (NRL), 2007. Enhanced UXO Discrimination Using Frequency-Domain Electromagnetic Induction, Final Report ESTCP MM0033.
- Prouty, M., George, D.C., and Snyder, D.D., 2011. MetalMapper: A Multi-Sensors TEM System for UXO Detection and Classification, Final Report ESTCP MR0603.
- Steinhurst, D.A., Harbaugh, G.R., Kingdon, J.B., Furuya, T., Keiswetter, D.A., and George, D.C., 2010. EMI Array for Cued UXO Discrimination, Final Report ESTCP MM0601.

This page left blank intentionally.

APPENDIX A
POINTS OF CONTACT

Point of Contact	Organization	Phone Fax E-Mail	Role In Project
T. Jeffrey Gamey	Battelle 100A Donner Drive Oak Ridge, TN 37830	Phone: (865) 599-0820 E-Mail: gameytj@battelle.org	Geophysicist – Principle Investigator
William Doll	Battelle 100A Donner Drive Oak Ridge, TN 37830	Phone: (865) 599-6165 E-Mail: dollw@battelle.org	Geophysicist – modeling assessment, data collection, data analysis
Scott Holladay	Geosensors 66 Mann Avenue Toronto, ON M4S-2Y3 Canada	Phone: (416) 483-4691 E-Mail: scott.holladay@geosensors.com	Geophysicist – array design and construction, electronics support, data analysis
Bruce Barrow	Leidos (formerly SAIC) 4001 North Fairfax Drive Arlington, VA 22203	Phone: (703) 276-4804 E-Mail: bruce.j.barrow@leidos.com	Geophysicist – modeling and inversion
Robert Selfridge	Corps of Engineers 4820 University Square Huntsville, AL 35816-1822	Phone: (256) 895-1887 E-Mail: bob.j.selfridge@hnd01.usace.army.mil	Geophysicist – autonomous platform integration, ground truth support

This page left blank intentionally.



ESTCP Office

4800 Mark Center Drive
Suite 17D08
Alexandria, VA 22350-3605

(571) 372-6565 (Phone)

E-mail: estcp@estcp.org
www.serdp-estcp.org